

THE PENNSYLVANIA STATE UNIVERSITY
SCHREYER HONORS COLLEGE

DEPARTMENT OF ENERGY & MINERAL ENGINEERING

CONCENTRATION-DISCHARGE RELATIONS IN CONNECTION WITH
END-MEMBERS AND FLOW PATHS, IN A MODEL CATCHMENT

SRUTHI KAKUTURU
SPRING 2017

A thesis
submitted in partial fulfillment
of the requirements
for a baccalaureate degree
in Environmental Systems Engineering
with honors in Environmental Systems Engineering

Reviewed and approved* by the following:

Li Li
Associate professor in the Department of Civil & Environmental Engineering
Thesis Supervisor

Mark Klima
Associate Professor of Mineral Processing and Geo-Environmental Engineering
Honors Adviser

* Signatures are on file in the Schreyer Honors College.

ABSTRACT

The goal of this research is to characterize concentration (C) – discharge (Q) relations for the species F^- , Br^- , Cl^- , NO_3^- , SO_4^{2-} , Na^+ , Mg^{2+} , Ca^{2+} , K^+ , pH and Dissolved Organic Carbon (DOC). Understanding CQ relationships are important for estimating solute and contaminant loads to rivers and streams and ultimately to the ocean. It also enables understanding of two overarching concepts: Flow Paths and End Members of chemicals. This experiment was performed in a physical model catchment (approximately 40 X 80 cm in area) resembling the real watershed Susquehanna Shale Hills Critical Zone Observatory (SSHCZO, 0.08 km²). The model catchment was 3D printed using the elevation and topographical data, soil from the real catchment was packed, and sprinkling experiments were conducted to simulate large rainfall events. The discharge from the model watershed was collected and analyzed to quantify water quantity and chemical composition. The advantage of the approach is that although soils are from a real watershed, the processes are not affected by ecological and microbiological processes at the watershed. With a deep groundwater component, the stream discharge primarily comes from two end members: rain fall with new water composition C_{new} and soil water C_{old} . Three patterns of end member contribution were characterized. F^- fell into Type A species, where rainfall is the dominant end-member and soil buffers the discharge load by retaining these species. Br^- and NO_3^- fell into Type B species, where discharge load is similar to input load, therefore soil is neither dissolving nor retaining these species. Cl^- , Ca^{2+} , K^+ , Na^+ , Mg^{2+} and SO_4^{2-} all fell into Type C species, where soil was the significant end member, and the soil gradually leached out these stored species during rainfall events with concentrations much larger than the rainfall input. Hysteresis patterns roughly show that F^- mimicked chemodynamic behavior. Br^- , Cl^- , Ca^{2+} , K^+ show dilution behavior. Na^+ , Mg^{2+} and pH show chemostatic behavior. And NO_3^- , SO_4^{2-} and DOC show crisscross CQ patterns that are in essence, chemostatic. These patterns together suggest that C_{old} is larger than C_{new} for the most part, meaning the discharge load synchronizes itself with soil water composition. Time along each Run has the influence of connecting pores so that old water contribution can increase over the course of a precipitation event. Insights gained here will facilitate grouping of

different behaviors of chemicals from different sources and predict solute loads and water quality in aquatic systems.

TABLE OF CONTENTS

LIST OF FIGURES	iii
LIST OF TABLES	iv
GLOSSARY	iv
ACKNOWLEDGEMENTS	v
Chapter 1 : INTRODUCTION.....	1
Catchment Hydrology	2
Coupling Factors	3
Questions to Address.....	5
Chapter 2 : METHODOLOGY.....	7
Model Catchment and Sprinkling Experiment.....	7
Building the 3D model	8
Model Setup	10
Soil Parameters and Packing	12
Precipitation –Rates and Composition	15
Experimental Design.....	18
Water and Chemical Balance Calculations	19
Chapter 3 : RESULTS & DISCUSSION.....	22
Water and Chemical Balance	22
Chemical Mass Balance	23
Soil Leaching Batch Experiments	25
Discharge Data.....	26
Run 1 Observations	29
Run 2 Observations	31
DOC and pH.....	33
End Member Mixing Analysis	34
Hysteresis Patterns	36
Classification.....	38
Chapter 4 : CONCLUSION	40
BIBLIOGRAPHY	41
APPENDIX.....	44

LIST OF FIGURES

Figure 1: Discharge Components in Real Watershed	2
Figure 2: CQ Hysteresis Patterns (Evans et al, 1998).....	4
Figure 3: Susquehanna Shale Hills Critical Zone Observatory	7
Figure 4: Solid Works Model Design	9
Figure 5: Building bedrock of model.....	10
Figure 6: Finished bedrock of model	10
Figure 7: Rain Simulation Setup.....	11
Figure 8: Overall Setup.....	12
Figure 9: Soil drying after field collection.....	13
Figure 10: Particle Size Distribution.....	13
Figure 11: Precipitation Trend	15
Figure 12: Frequency of precipitation rate.....	16
Figure 13: Preparing rainwater	17
Figure 14: Precipitation Schedule	18
Figure 15: Precipitation Pattern in Run 1 and 2.....	19
Figure 16: Discharge Components in Experiment.....	20
Figure 17: C and Q (horizontal gridlines are for Conc. right axis).....	27
Figure 18: Ratios and Q (horizontal gridlines are for Conc. right axis).....	28
Figure 19: 20X Ratio-C Patterns.....	32
Figure 20: C and Q –part 2 (horizontal gridlines are for Conc. right axis).....	33
Figure 21: 1-dimensional EMMA for Run 1	35
Figure 22: C-Q Graphs -Hysteresis Loops.....	36

LIST OF TABLES

Table 1: Scaling Parameters.....	14
Table 2: Soil Packing Parameters of the model watershed	14
Table 3: Rainwater Composition	17
Table 4: Volume Balance Totals.....	22
Table 5: Mass Calculations R1	23
Table 6: Mass Calculations R2	23
Table 7: Batch Experiment Results.....	25
Table 8: Calculations/Values for Mixing Diagram.....	34
Table 9: Hysteresis Summary	37
Table 10: Experiment Observations Summary	38

GLOSSARY

Adsorption

A smaller molecule attaching onto the surface of soil.

Catchment / Watershed

Fundamental hydrogeological unit where a water balance can be applied

Discharge

Volumetric flow rate of water that is flowing out of a stream channel.

Dissolution

Molecules embedded in soil particle matrix or on its surface end their attachment with soil and dissolve into the bulk of the fluid (water) solution

End-Member

Source of chemical load to stream discharge

First-Order Catchment

Catchment of a first-order stream, which is a head-water tributary (no other streams to “feed” it) and ultimately connecting into larger streams.

Hydrograph

Discharge rate of stream over time, often showing the aftermath of a precipitation event.

Hyetograph

Volume or length of precipitation over time in a particular area.

Hysteresis

“the phenomenon in which the value of a physical property lags behind changes in the effect causing it, as for instance when magnetic induction lags behind the magnetizing force.”

Hysteresis loop

A positive trend between two variables turning negative over time, or vice-versa.

Residence Time

Length of time that a travelling water molecule stays in the system of study.

Retention

Soil keeps molecule by taking it out of solution and onto the soil matrix or surface (opposite of dissolution)

Turbidity

Measure of opaqueness of water. Lighter water is less turbid.

ACKNOWLEDGEMENTS

Zhang Cai, *Ph.D. Candidate*

Wei Zhi, *Graduate Student*

Dacheng Xiao, *Graduate Student*

Laura Leirmann

Carol Confer

Chapter 1 : INTRODUCTION

Studying how water routes through a watershed and how it carries nutrients are important in estimating nutrient load to natural water systems, and potentially to address problems such as eutrophication (presence of excess nutrients in surface waters) and fertilizer runoff from agricultural lands. Nutrient transport is important to city planners and environmental engineers as well, who may need to map floodplains, make infrastructure decisions, analyze or predict the impact of human activities or impact to humans etc. For instance, understanding the effects of acid rain on stream pH involves understanding soil-water interactions. As acidic rain falls on a catchment, the stream pH is expected to decrease. However, even as rain stops, the stream pH continues to decrease, which could be explained by water gaining more acidic chemical composition at the soil-water interface [Hornberger, 2014]. Besides pH, there are other chemicals whose concentrations need to be kept below a certain acceptable level in streams. Studying how rain and snow affect discharge rates of a river and the concentration of chemicals or components it carries is important to maintain river and ecosystem health.

Also in the natural world, soil, rock and minerals slowly go through weathering and erosion processes. Weathering breaks down sediment both chemically and physically, and is an important process in forming soil. Erosion is responsible for transporting the soil and its constituents. In a watershed, these may be eroded into the river channel. These processes are influenced by several factors such as parent material, climate, organic matter, topography and time. A major driver of weathering and erosion is water, through the process of precipitation. Rainwater is naturally acidic and it mimics the chemical composition of its surroundings (i.e. rainwater near the sea has more chloride because it originates from evaporated sea water, which contains chloride ions). This acidic and concentrated concoction is useful in dissolving the soil which it falls on, and to leach out chemicals from its surface and layers. It is worthwhile to study how the intensity of precipitation can influence soil erosion and nutrient load transport. Many climate change models predict that some areas of the world may experience higher intensity rainfall events and more

mean precipitation as the earth warms [“Floods and Droughts”]. The question remains of whether these changes affect soil erosion and nutrient load transport.

Catchment Hydrology

Geochemical, hydrological, physical and biological processes in a catchment interact to make up the dissolved load to its stream. The CQ (concentration-discharge rate) relations at the stream mouth reflect the characterization and coupling of some of those processes [Anderson, 1997]. One topic of importance within this realm is how precipitated water travels to the stream, characterized by flow components, summarized in Figure 1: Discharge Components in Real Watershed.

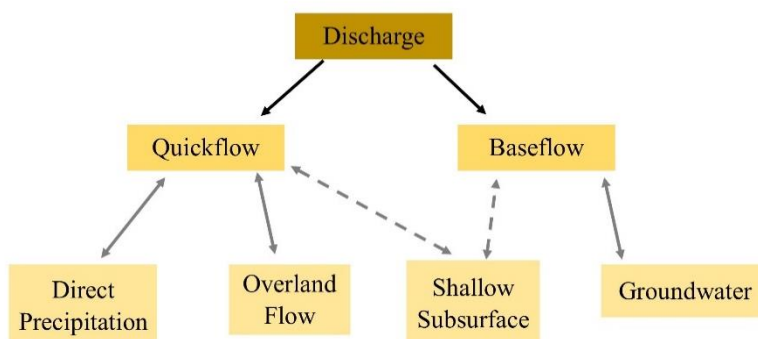


Figure 1: Discharge Components in Real Watershed

Stream discharge is the sum of two components: *quickflow* and *baseflow*. Quickflow is the contribution to discharge observed immediately after increased precipitation, and baseflow is the contribution to discharge that occurs after a time lag. The pathways of precipitated water can be one of four ways: *direct precipitation*, *overland flow*, *shallow subsurface flow* and *groundwater flow*. These pathways do not necessarily coincide to either the quick or subsurface flow category. However, direct precipitation and surface flow are often quickflow, and baseflow is often the saturated groundwater zone’s contribution to river discharge. Contribution of direct precipitation to discharge is often very small. Overland flow is a large factor, and its contribution can increase due to 1) impermeable surface (i.e.

concrete pavement) or 2) precipitation rate greatly exceeding infiltration rate, or soil is already fully-saturated [Hornberger, 2014].

Hydrologists have found it a challenge to separate, quantify and analyze discharge components because these concepts initiated empirically. Another way to continue our understanding is through “end member mixing analysis”, or EMMA, which uses chemistry to identify the source of water contributed to discharge and the chemical interactions it has gone through in its path. To conduct such a study, another classification for stream discharge is *new water versus old water*. New water is the discharge load with chemical composition similar to precipitation or event water itself. Old water, or “pre-event” water, is the water already in the soil being flushed into the stream. In temperate, forested catchments such as Shale Hills in central Pennsylvania, the vast majority of discharge into a stream after a precipitation event is old water [Hornberger, 2014].

Coupling Factors

Major chemicals in streams [Berner and Berner, 1987; Allan, 1995] are ions including HCO_3^- , Ca^{2+} , SO_4^{2-} , H_4SiO_4 , Cl^- , Na^+ , Mg^{2+} , K^+ , nutrients (N and P), dissolved organic matter (DOC), dissolved gases such as N_2 , CO_2 , O_2 , and trace metals. Some of the following calculations [Anderson, 1997] help to characterize basic relations between chemical and kinetic characteristics of a species.

Equation 1

$$Q_d C_d = Q_{old} C_{old} + Q_{new} C_{new}$$

Equation 2

$$X_{old} = \frac{C_d - C_{new}}{C_{old} - C_{new}}$$

Where, C and Q are concentration and discharge flow rate, respectively. Subscript *d* refers to the components of output discharge from the watershed, subscripts *old* and *new* refer to old and new water

components. C_{new} and Q_{new} are the same as C_p and Q_p , which are concentration and discharge rate respectively, of precipitation. X_{old} is the fraction of old water contributing to runoff. When X_{old} increases, concentration of species is generally higher because the water has had more time to interact with sediment. When subsurface flow dominates, more of the discharge is likely to be old water rather than new water [Wohl, 2014].

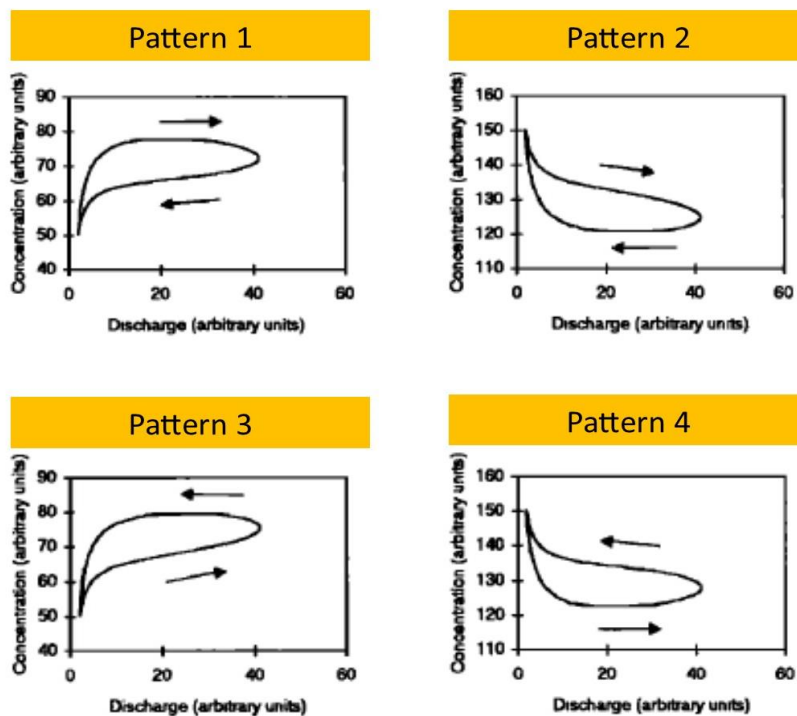


Figure 2: CQ Hysteresis Patterns (Evans et al, 1998)

C-Q relations can also follow hysteresis loops –when concentration differs along the rising and falling limbs of a hystograph [Walling and Webb, 1986]. When C_d is higher on the rising limb than on the falling limb of Q_d , a clockwise hysteresis loop is seen in a graph of concentration vs. discharge. When C_d is lower on the rising limb, a counterclockwise loop is seen. When the loop trend is positive concave (Pattern 1 and 3 in Figure 2), $C_{new} > C_{old}$ or $C_p > C_{old}$. When it is negative concave (Patterns 2 and 4), $C_{new} < C_{old}$ or $C_p < C_{old}$ [Evans et al., 1998]. These 4 patterns are appropriate for watershed analysis with 2 end members of interest: rain water and soil water.

Species that have positive correlation between C and Q are termed *chemodynamic*, ones with negative correlation are termed *dilution* species, and ones with no correlation are termed *chemostatic*. It is also possible that some species exhibit crisscross patterns (both chemodynamic and dilution behavior at various parts of the rain event). Patterns 1 and 3 roughly yield chemodynamic behavior, and patterns 2 and 4 roughly yield dilution behavior.

Hydrogen ion concentration typically increases with discharge, showing chemodynamic behavior. Chloride, sulfate and other aerosol and rain-deposited anions are often not correlated with discharge, showing chemostatic behavior [Anderson 1997]. Mg^{2+} , Na^+ as well as Si and other base cations and alkalinity derive from mineral dissolution or soil weathering, could show a variety of behaviors. Species with high intrinsic weathering rates yield toward chemostatic concentration-discharge relations, but it depends on transit time (or how much time the water has had to interact with soil) [Ameli, 2017]. For instance, minerals containing sodium and potassium tend to dissolve slower than those containing calcium and magnesium [Sverdrup, 1993]. This means that CQ relations for mineral-dissolution derived species depends on many factors and requires further investigation.

Biology heavily influences nitrogen and is taken up by roots and microbial matter, limiting the amount going into the river. While at the same time, fertilizer runoff increases nitrogen and phosphorus concentration in the water [Boyer et al., 2006]. Organic matter concentration is also influenced by biology, as well as climate, seasons and physical characteristics of the watershed [Thurman, 1985]. Such biologically important species show both chemodynamic and dilution behavior [Basu et al., 2010; Grimm et al., 2003; Sebestyen et al., 2008].

Questions to Address

Concentration-discharge and end-member relations for each major chemical species is extensively studied. However, these observations are often an outcome of multiple factors including

climate, biological conditions, land cover, and topography. It is important to separate the effects of geochemical factors from the influence of biological and ecological processes. In this thesis, the overall chemical signature of each major species will be identified in terms of 1) relationship to discharge 2) source or significant end-member of the chemical. The overarching question is: how does the watershed retain and release chemicals? And, what are the different categories of chemical signature that a species can be assigned to?

Chapter 2 : METHODOLOGY

Model Catchment and Sprinkling Experiment

The National Science Foundation (NSF) established the Critical Zone program to intricately study the zone of earth from the ground to bedrock, typically reaching the bottom of a groundwater zone. Through research, infrastructure, models and data, the program aims to study how components of the critical zone interact to ultimately support life on earth. Among the 10 sites across the United States set aside for this program, the Susquehanna Shale Hills Critical Zone Observatory (SSH CZO; Figure 3) is situated near Penn State -University Park. This CZO is a forested, first-order catchment over shale bedrock in temperate climate. There is a large database of quantified hydrological, geological and ecological processes, and the main emphasis is on “pathways and rates of water, solutes, and sediments”.



Figure 3: Susquehanna Shale Hills Critical Zone Observatory

This project involves *quantifying nutrient transport and C-Q (concentration, C and discharge, Q) relations in a smaller, simplified and controlled physical model watershed* in the laboratory, and using the CZO database for comparative analysis. A bedrock outline (about 80x40 cm) of this catchment was 3D

printed, soil representative of the real catchment was packed. Sprinkling experiments were conducted to represent large rainfall events. The discharge from the model watershed was collected and analyzed to quantify C-Q relationships relating to water path and EMMA concepts.

Because a real watershed is dynamic and intricate the model does not represent the actual CZO in terms of realistic quantification of concentration and how it relates precipitation and discharge as it does not include the effects of vegetation, seasons, human influences on land etc. However, this 3D model was built to separate variables and to focus on the geochemical, but not biological or ecological aspects of solute transport and CQ relations. This is comparable to the purpose of a flow cell, which is typically meant for subsurface studies. In this miniature CZO model, a controlled experiment was conducted that singled out the factor of sedimentary composition to study CQ and EMMA. After understanding the mechanisms that precipitated water used to end up as discharge, the whole process was further analyzed. This research project also analyzed the variable of precipitation composition, and how it relates to the concepts of solute transport.

Building the 3D model

The outline and rough topography of SSH CZO was utilized in building the bedrock container that held the watershed, along with a wall to contain the soil. Ideally, shale rock would have been used to chisel it to desired shape. We ultimately decided that Penn State's 3D printing resources should be used to build a small scale box. The shape of the model was built in SolidWorks (Figure 4). The model CZO shape and relative dimensions (length, width and area) are to reflect the actual contour and profile of the real CZO.

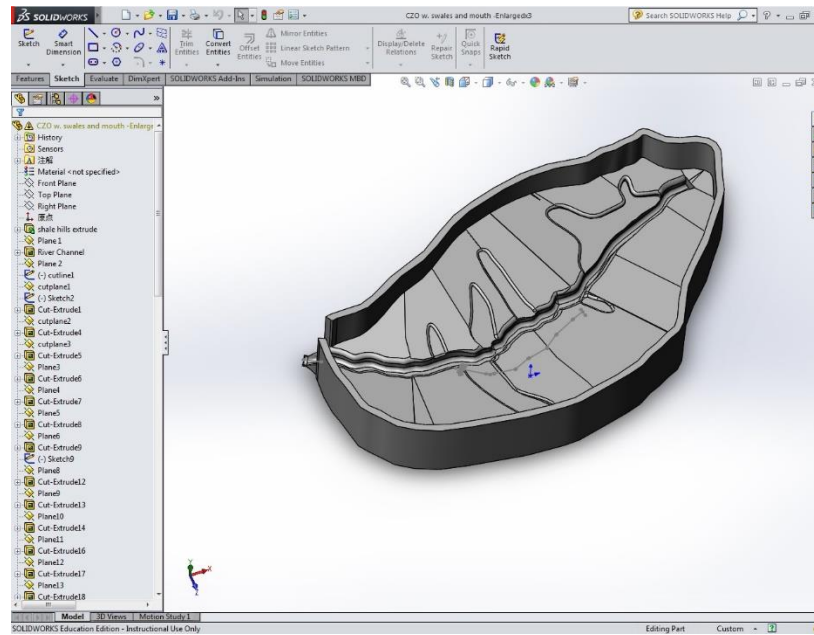


Figure 4: Solid Works Model Design

The model was printed in 16 pieces (since the 3D printer has maximum dimensions much smaller than the real watershed size) and were glued together using strong non-reactive silicon adhesive (Figure 5). The final watershed measures 40 by 80 cm in area. Since the larger-model prints were more porous due to our large 3D material demand, the model needed to be made non-porous in order to reflect the purpose of a shale bedrock and to create a closed and controlled system. To achieve this, the model was covered with non-reactive yellow cellophane plastic using silicon adhesive below and above it to further seal it and make it water resistant. At the river channel, we used more silicon adhesive and no plastic because its curvature made it difficult to wrap plastic around (Figure 6).



Figure 5: Building bedrock of model

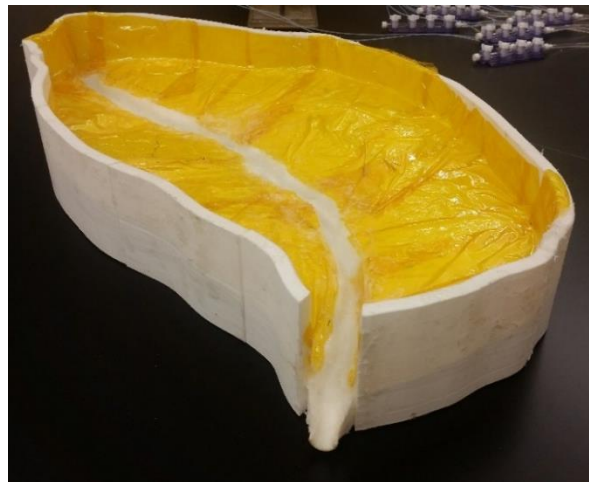


Figure 6: Finished bedrock of model

Model Setup

To simulate rain fall on, a peristaltic pump was used to sprinkle rainwater on the catchment at specific rates. Artificially made rainwater was placed in a large glass beaker, from which 8 tubes were placed. These tubes went through the pump, and then manifolds were used to distribute the water from each tube into 2 or 4 smaller tubes, totaling 30 outlets for the rainwater. At the outlets, a screw was attached to the edge of the small tubes in order fix them all to the rain plate which contained 30 holes. This plate was chiseled and drilled by a workshop and was created in the shape of the 3D model in order

to be placed above it (Figure 7). The large number of rainfall outlets was used to even out the spatial distribution of the rain fall.

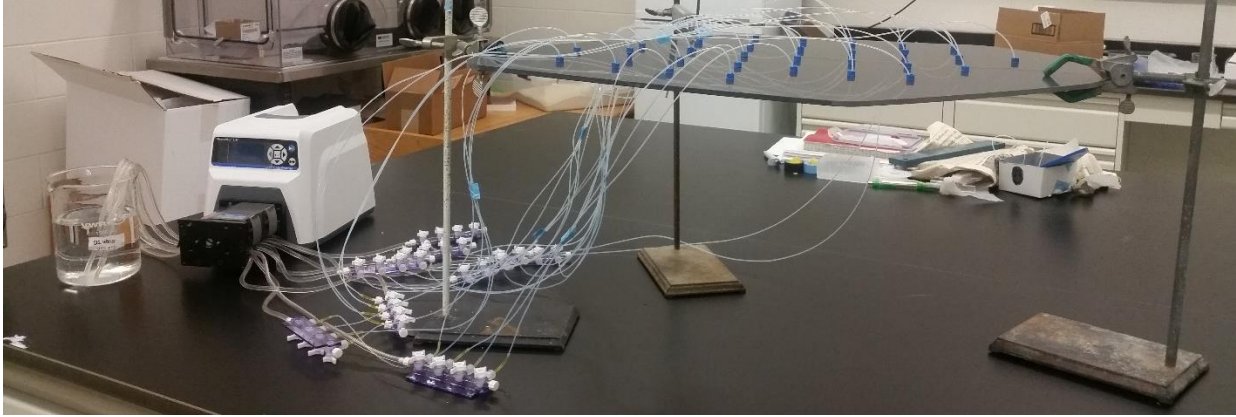


Figure 7: Rain Simulation Setup

The SSHCZO has a 6.35° angle from the valley floor to the ridge top (Bao et. al., 2016). A cardboard structure was created to make the ridge top sit 8.9 cm higher than the front edge (Since the length of model is 80 cm, $\tan^{-1}(8.9/80)$ to approximate the 6.35°). The cardboard structure was stuffed with paper to give it rigidity, and then covered up. The 3D printed model with packed soil was placed on top of this angled creation. Clamps were used to hold the rain plate in place, and this was also angled. Overall setup can be seen in Figure 8. Discharge was collected with the help of a (yellow) funnel, into tubes placed in an automatic tube collector at specified time intervals.

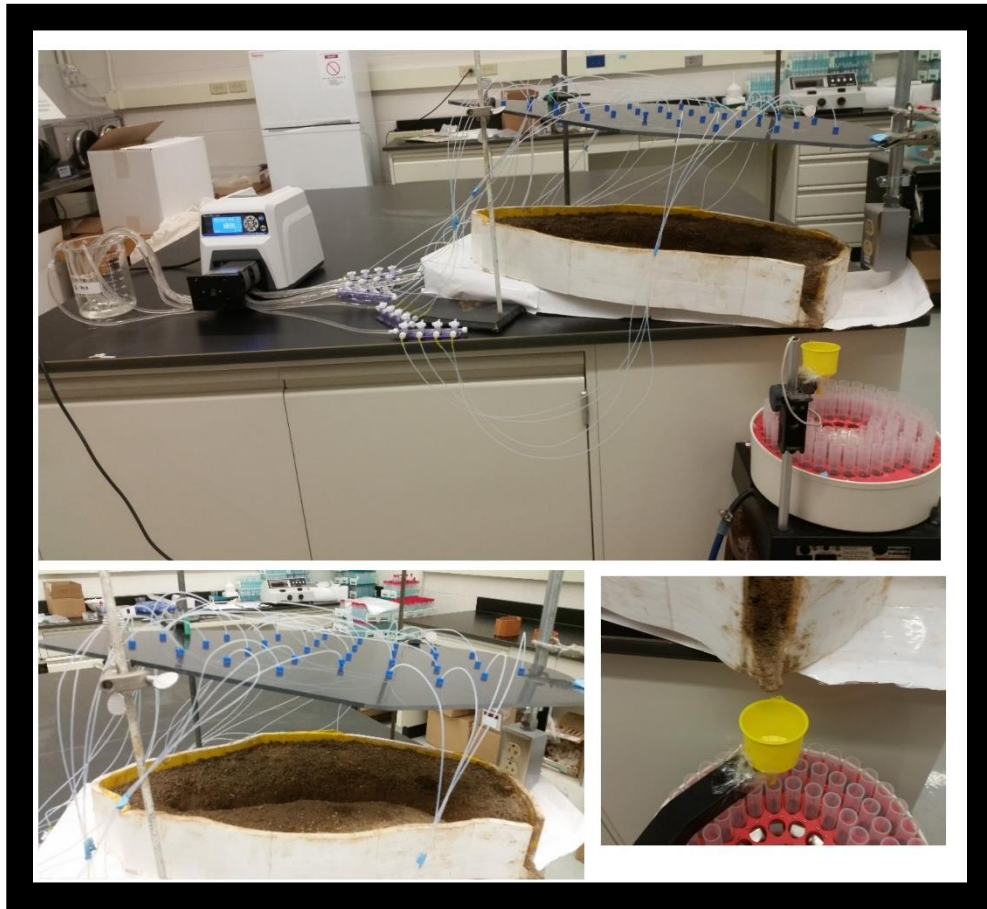


Figure 8: Overall Setup

Soil Parameters and Packing

Soil from the SSH CZO was collected to pack in the 3D model. Soil in the CZO has 4 layers, the 0-5 cm layer, 5-15 cm layer, 15-30 cm layer, and 30-50 cm layer. Typically the organic matter decreases at deeper soils. Soil was collected from each layer, kept in plastic bags, taken to the lab and then laid out on newspapers to dry completely (Figure 9). After drying, particles larger than 2 mm were screened out due to our prediction that they may be inappropriately sized for the small model. Also, selecting a certain size range allowed for more precisely analysis. Full screening of the particles smaller than 1180 μm yielded the particle size distribution shown in Figure 10. Soils was difficult to pack when dry, because it

slipped into the river channel that needed to be kept relatively clean, in order to study the properties of the effluent water without suspended particles. Therefore, soil was packed wet. Particle range of 106 to 2000 μm was used for the experiment.



Figure 9: Soil drying after field collection

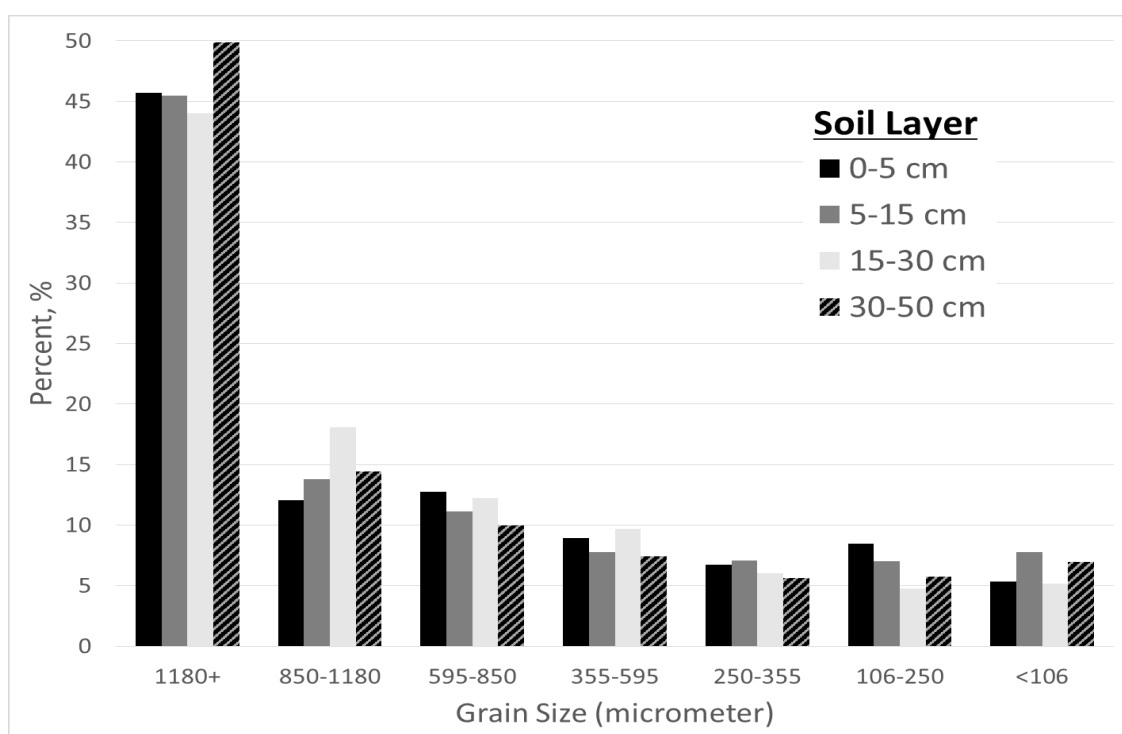


Figure 10: Particle Size Distribution

By scaling down parameters, amount of soil needed was calculated as follows:

Table 1: Scaling Parameters

	<u>Actual</u>	<u>Accurate Model</u>	<u>Actual Model</u>
Soil Depth to bedrock (m)	0.95	0.001407 ¹	0.03
Length CZO (m)	540	0.8	
Width CZO (m)	313	0.4	
Area, CZO (m ²)	168,750	0.32	0.158
Volume, Total (m ³)	160,313	0.00045	0.00477 ²

¹Calculation: Based on length ratio [0.8/540] times the average real depth 0.95 m

This depth is unrealistic and needs to increase for two reasons. Soil cannot be packed this thin, and it would not be possible to conduct a reactive transport experiment on the material, as the soil will easily wash off. Rather, an average depth of 4 cm was chosen because it would be realistic and also appropriate for the 3D printed model which has a height of 4-5 cm at the ridge top. Only the average height was included, because at this scale and loose packing given the situation, accurate layers cannot be achieved. However, soil was packed more toward the channel and less toward the ridge top.

²Calculation: Based on the soil depth used, times the area of CZO model, total soil volume (with pores) was found.

Table 2: Soil Packing Parameters of the model watershed

Parameter		Calculations
Soil Volume (cm ³)	2861	¹
Pore Volume (cm ³)	1908	
Soil Weight (g)	7584	²
Wt. Layers: 0-5 (10%)	758	³
5-15 (20%)	1517	
15-30 (30%)	2275	
30-50 (40%)	3034	

¹Calculation: $0.00477 \text{ m}^3 * (100^3 \text{ cm}^3/\text{m}^3) * (1-0.4)$ where 0.4 is porosity

Since SSH CZO soil is generally of silty loam inceptisol category, porosity is approximated at 0.4 based on convention ("Swiss Standard").

²Calculation: Using average particle density of such soil: 2.65 g/cm³, multiplied density and volume to get mass of soil.

³Calculation: Since particle density is assumed to be constant, percentage of each layer was used to calculate soil weight (in grams) needed to be measured and packed in the CZO model. Soil was weighed accordingly.

Precipitation –Rates and Composition

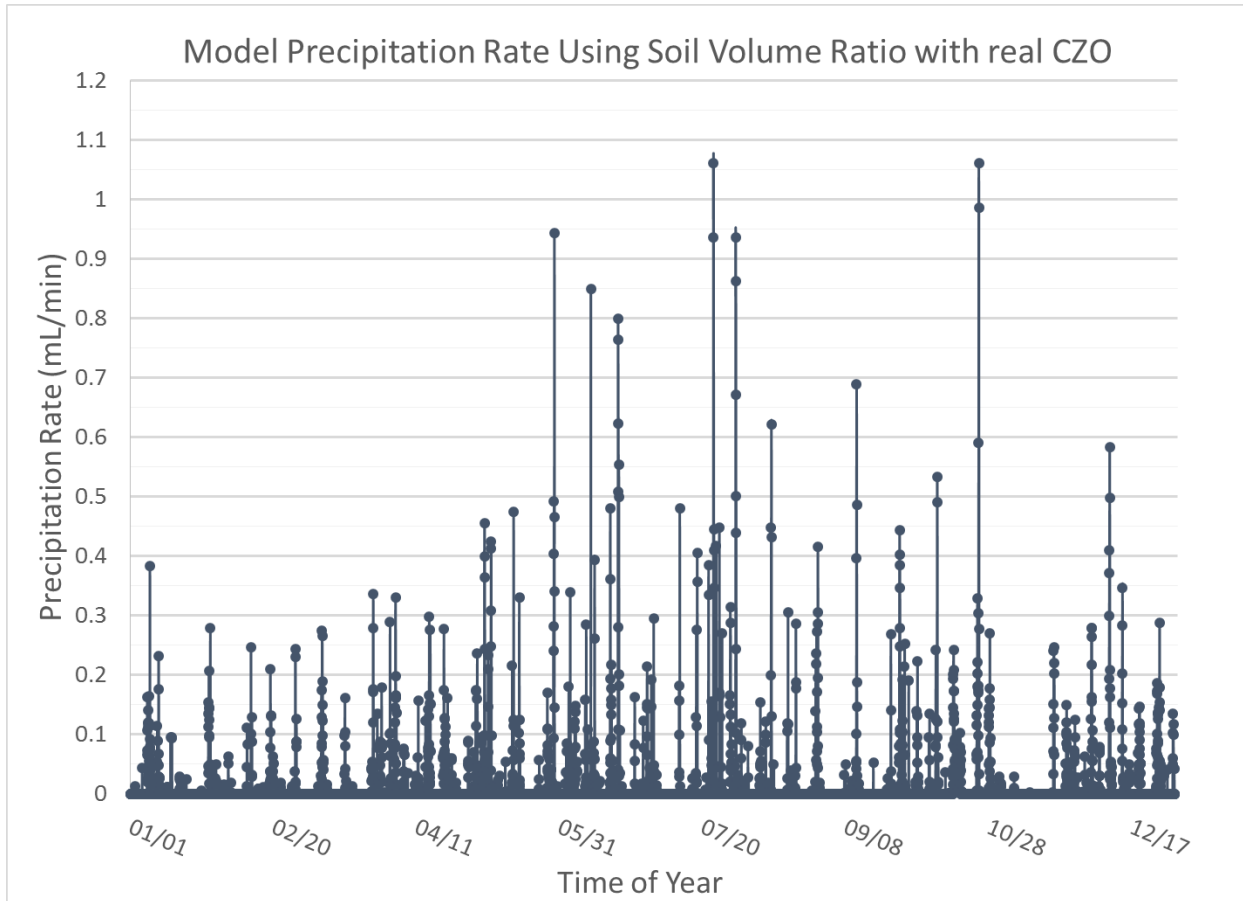


Figure 11: Precipitation Trend

To calculate appropriate rainfall rates for the experiment, hourly precipitation (m/day) on SSH CZO was scaled down to the model through the following calculations:

$$\text{Volumetric Precipitation in Model} = \frac{m}{\text{day}} * \frac{1d}{1440 \text{ mins}} * \frac{168750 \text{ m}^2}{1} * \frac{10^6 \text{ ml}}{\text{m}^3} * \frac{0.00477}{160313}$$

where $\frac{0.00477}{160313}$ is the soil volume ratio between the model and real watershed. Figure 11 shows the 2009 precipitation rates scaled down to the CZO model. Figure 12 is the frequency graph for those rates.

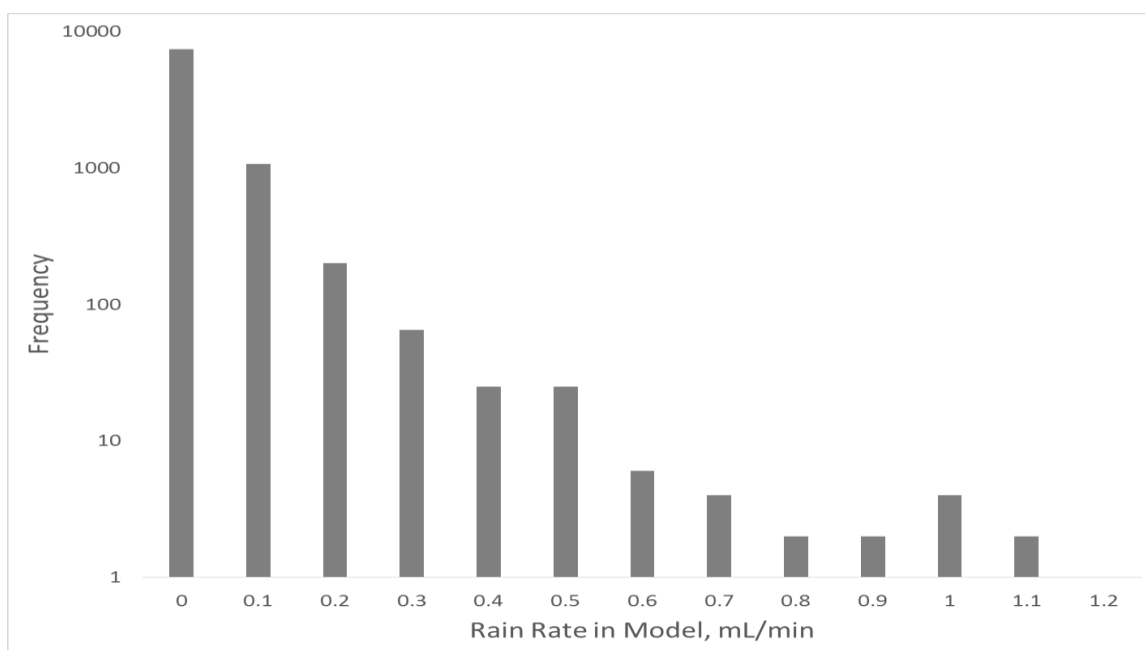


Figure 12: Frequency of precipitation rate

The rainfall rates vary up to 1.1 mL/min. The most frequent rate is rate is 0.1 mL/min. This rate however, is too small for the peristaltic pump to pump up water. A slightly higher set of flow rates ranging up to 1.5 mL/min were selected for rain simulation (discussed in next section).

A rate of 1.5 mL/min translates to $\sim 9.5 \mu\text{m}/\text{min}$ over the area of the model watershed. However, this is misleadingly small because the soil packing height is much larger than a realistic scaled down height. Since the soil volume ratio was used to calculate this rain simulation flow rate, this rate is appropriate for the amount of soil packed (although larger).

Artificial rain was created using the rainfall composition data of 2009 from SSH CZO online database. It was made to contain the composition summarized in Table 3 and an average pH of 4.98. The right side of Table 3 shows chemical compounds and acids that were used to achieve that chemical composition. One liter of 400 times concentrated solution was made by adding required weight of compound and acid to pure de-ionized (DI) water, since it was easier to weigh the constituents this way. After using a magnetic stirrer to mix (Figure 13), this concentrated solution was then diluted to 1X rain water and also to 20X rain water in a different beaker. Their pH was measured and recorded periodically.

The actual concentration of the rain water was measured later and those values were used for analysis instead of intended concentration shown in Table 3.

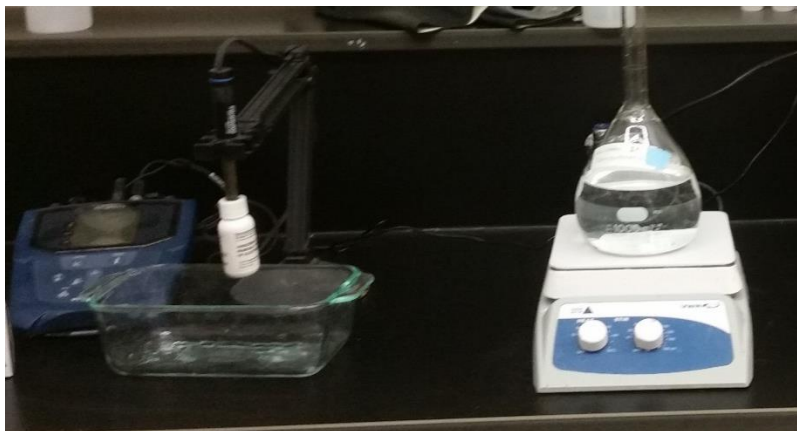


Figure 13: Preparing rainwater

Table 3: Rainwater Composition

Ions	ppm		Chemical	ppm	400 times (mg/L)
Ca ²⁺	0.109		Ca(Cl) ₂	6.05E-02	24.2
Mg ²⁺	0.017		Ca(NO ₃) ₂	3.58E-01	143.0
K ¹⁺	0.021		MgCl ₂	6.73E-02	26.9
Na ¹⁺	0.046		KCl	4.01E-02	16.0
NH ₄ ¹⁺	0.258		Na ₂ SO ₄	1.42E-01	56.8
NO ₃ ¹⁻	0.967		(NH ₄) ₂ SO ₄	9.46E-01	378.4
Cl ¹⁻	0.108		HNO ₃	7.08E-01	283.2
SO ₄ ²⁻	1.242		H ₂ SO ₄	4.67E-01	187.0

Experimental Design

The overall experimental schedule is shown in Figure 14. First, the experiment started off with an “initial flush”, where small particles were expected to wash out, and soil parameters would begin to stabilize. Wash load is the finest of sediment particles flushing out of a watershed land and into a stream, because the force of precipitation overcomes their low settling velocity [Wohl, 2014]. The Initial Flush was done at Q_p of 1.5 mL/min for 17 hours.

After observing the effluent turbidity and color stabilizing during the initial flush, the “background phase” was started. This was to prevent the model catchment from drying to a point where pore spaces collapsed and messed with the equilibrium that soil had reached. This was done at the rate of 0.1 mL/min for 26 hours between Initial Flush and Run 1, and 170 hours between Run 1 and 2. Run 1 and 2 were the main “Rain Event Simulations”, hereon referred to as R1 and R2.

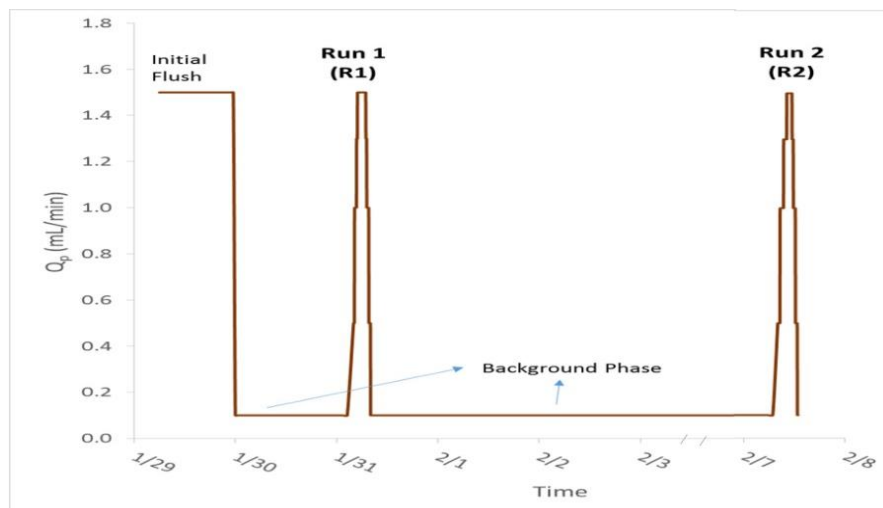


Figure 14: Precipitation Schedule

In R1 and R2, Q_p was incrementally increased from 0.1 to 0.5 to 1.0 to 1.3 to 1.5 mL/min, as shown in Figure 15, which contains magnified parts of Figure 14. In R2 of each experiment, 20 times

concentrated rain water was used for the peak rate of 1.5 instead, but the same rate pattern was kept. This was to see the effects of concentration-discharge and end members at a magnified scale.

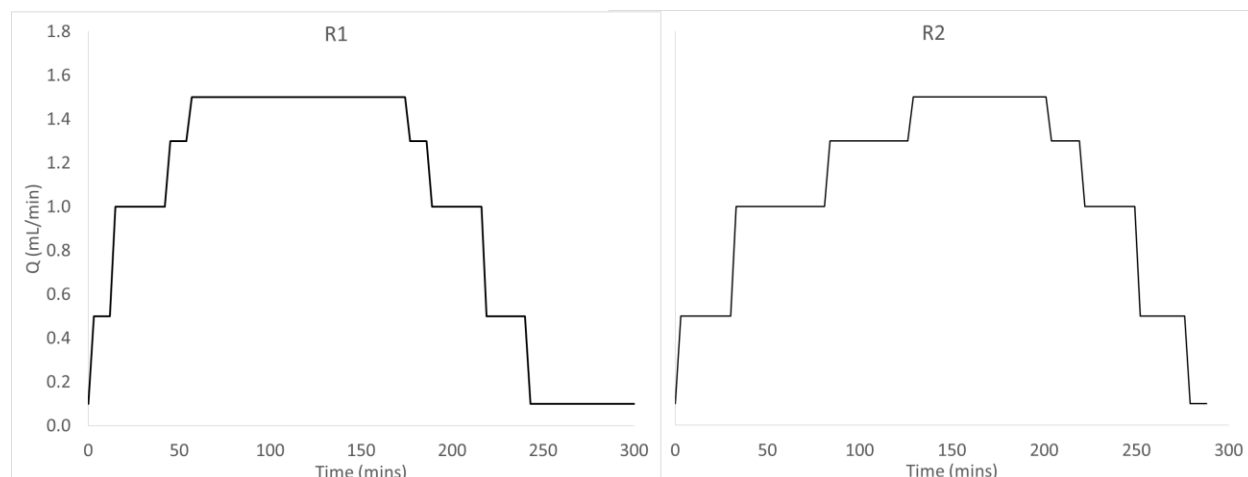


Figure 15: Precipitation Pattern in Run 1 and 2

As rain fell on the model, the river mouth discharged water, and these effluent samples were collected at interval of 3 minutes using an automatic sample collector. These samples were measured for pH immediately, and later for their anion, cation and DOC concentrations. Anions were measured using the Ion Chromatography machine and cations using the Mass Spectrometry machine. Batch experiments were also conducted to see how soil leached out chemicals.

Water and Chemical Balance Calculations

For this experiment, discharge components have been simplified into two parts, as shown in Figure 16. We have the rainfall and soil water components however not deeper groundwater. Direct precipitation into stream is insignificant, both in the real watershed and especially in the model for this experiment. Therefore, the components of overland and subsurface flow remain. New and old water are two parallel component classification of discharge load. However, they do not always coincide respectively with the components of overland and subsurface flow.

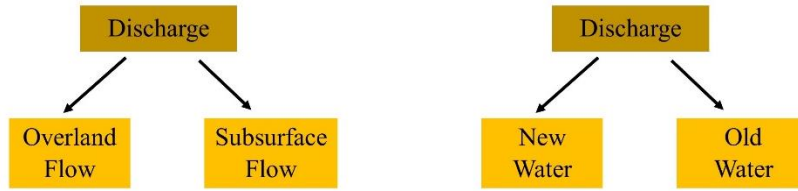


Figure 16: Discharge Components in Experiment

To analyze the end-members and concentration, following calculations were made:

Equation 3: Volume Ratio

$$R_V = \frac{V_d}{V_p}$$

Equation 4: Total Volume Ratio

$$R_{TV} = \frac{V_{d-total}}{V_{p-total}}$$

Equation 5: Concentration Ratio

$$R_C = \frac{|C_d - C_p|}{C_d}$$

Equation 6: Volumetric Balance

$$V_p = V_{ET} + V_d + V_s$$

Where, V_p , V_{ET} , V_d , V_s is volume of precipitation (input), evapotranspiration, discharge (output) and water storage in soil, respectively. V_v , not mentioned, is the total pore volume. $V_{d-total}$ and $V_{p-total}$ in Equation 4 is the total volume collected and inserted in one run, respectively. C_d is concentration of a particular chemical in discharge (output) and C_p is concentration in precipitation (input). C_p is assumed to be the same as C_{new} .

R_V reflects the volume of water that comes out of the watershed with respect to what is input. If the ratio is small, there is potentially more water retained in the soil, which could later yield old-water contribution. A high ratio means that discharge is dominated by overland flow, and the water has spent less time with the soil. Since there is a time lag for Q_d to respond to Q_p , it is also necessary to look at the overall volume ratio, R_{TV} . It quantifies how much water the catchment can hold in an event and leads to

further understanding of its relationship to concentration. R_C helps identify the source of chemical load coming out of the watershed and corresponds to old water contribution.

For $R_C = 1$, there is no contribution from C_p and the load is coming from soil-water interface, possibly with help of old water contribution

For $R_C > 1$, C_d is much lower than C_p , meaning retention /buffering is involved.

For $R_C < 1$ or close to 0, C_d is similar to C_p , rain water is the main source of loading.

Mass Balance calculations were also made:

Equation 7: Volume Ratio

$$M = \sum C_i Q_i t_i$$

Where C_i , Q_i and t_i refer to concentration, discharge and time of each measurement interval respectively, and M (mass of a chemical in a Run) is the sum of all intervals. M_{in} and M_{out} , the total mass input and output for each Run for each chemical were calculated. $\Delta M (= M_{out} - M_{in})$ was also calculated. $\Delta M/M_{in}$ (ratio) and $\Delta M/\Delta t$ (where Δt is the overall time of the Run) were also calculated.

To understand how and to what extent each species dissolves from soil, batch experiments were conducted. In 2 vials, 1 gram of soil was placed in 10 mL (gram) of DI water. These samples were shaken and kept for 2 hours each and 18 hours, after which they were filtered so the soil cannot dissolve more chemicals. The same process was repeated for prepared rain water, for a total of 4 batch experiment results, summarized in Results Section.

Chapter 3 : RESULTS & DISCUSSION

Water and Chemical Balance

Table 4: Volume Balance Totals

[cm ³]	Whole Exp.*	Whole Exp.*	Run 1	Run 2
V _{p-total}	3800		310	305
V _{d-total}	1100		170	260
V _s [*]	1908**	50%**		
V _{ET} ^{**}	792***	20%***		
V _{d-total} /V _{p-total}		30%	55%	85%
V _{p-total} /V _{v-total}			16%	

*Whole Experiment is both runs and background phases.

**This is the potential maximum V_s value, which is equal to the total pore volume, V_v at full saturation. However, the catchment is not always fully saturated.

***Minimum V_{ET} calculated using Equation 6.

For comparison, V_{p-total}/V_{v-total} in real CZO watershed was calculated.

$$\frac{V_{p-total,real}}{V_{v-total,real}} = \frac{1.75 \text{ m}/365\text{days}^*}{160313 \text{ m}^3 \text{ catchment}} \times \frac{168750 \text{ m}^2 \text{ area}}{0.4 \text{ porosity}} = 4.6 \%$$

* Mean annual precipitation (MAP) is approximately 100 cm (“Annual Precipitation”).

V_{p-total}/V_{v-total} ratio for the model watershed was 16% (from Table 4) which is much higher than 4.6% for the real watershed (calculated above). A model ratio of 16% is an overestimation because it accounts for only the event itself, and skews the V_p input volume toward higher values. The real MAP accounts for all precipitation events, including small ones. Nevertheless, these ratios indicate that this model and sprinkling experiments simulate a precipitation event with increased intensity. V_{d-total}/V_{p-total} (Ratio_{TV}) increased from 55% in R1 to 85% in R2. This increase is because Run 2 was performed several days after Run 1, which allowed excess saturation to accumulate over time and possibly contribute to more overland flow and less old-water dominance. In this experiment, V_s for each Run cannot be calculated accurately because the water content in the soil was not measured. Run 2 probably has a lower

V_s out of the water that comes from its V_p . However, water stored in the model catchment prior to Run 2 is higher than that stored prior to Run 1.

Chemical Mass Balance

Table 5: Mass Calculations R1

<i>[μg]</i>	F ⁻	Br ⁻	Cl ⁻	NO ₃ ²⁻	SO ₄ ²⁻	Mg ²⁺	Na ⁺	Ca ²⁺	K ⁺
M _{in}	96.30	21.18	45.25	478.83	301.38	5.14	62.80	63.01	29.16
M _{out}	8.00	20.87	457.29	425.39	1431.10	131.03	275.76	317.69	549.58
ΔM	-88.30	-0.31	412.04	-53.44	1129.72	125.88	212.96	254.67	520.41
$\Delta\text{M}/\text{M}_{\text{in}}$ (ratio)	-0.917	-0.015	9.106	-0.112	3.748	24.470	3.391	4.042	17.846
$\Delta\text{M}/\Delta\text{t}$ ($\mu\text{g}/\text{min}$)	-0.225	-0.001	1.051	-0.136	2.882	0.321	0.543	0.650	1.328

Table 6: Mass Calculations R2

<i>[μg]</i>	F ⁻	Br ⁻	Cl ⁻	NO ₃ ²⁻	SO ₄ ²⁻	Mg ²⁺	Na ⁺	Ca ²⁺	K ⁺
M _{in}	58.01	19.62	240.10	2286.78	2965.30	25.21	1100.71	246.03	135.09
M _{out}	9.95	26.98	651.78	1262.68	2731.74	177.04	576.71	440.84	708.32
ΔM	48.07	7.36	411.68	1024.10	-233.56	151.83	-524.01	194.81	573.23
$\Delta\text{M}/\text{M}_{\text{in}}$ (ratio)	0.829	0.375	1.715	-0.448	-0.079	6.022	-0.476	0.792	4.243
$\Delta\text{M}/\Delta\text{t}$ ($\mu\text{g}/\text{min}$)	0.167	0.026	1.429	-3.556	-0.811	0.527	-1.819	0.676	1.990

Run 1 Observations

Positive ΔM indicates that soil releases that species significantly, which was the case for most species Cl⁻, SO₄²⁻, Mg²⁺, Na⁺, Ca²⁺ and K⁺. Negative ΔM indicates that the soil retains these species so that not all precipitation mass is released out of the watershed, which is the case for F⁻ and NO₃²⁻. ΔM close to zero means that input matches output and mass is almost balanced. This is the case for Br⁻, where ΔM is slightly negative but close to zero.

A high $\Delta M/M_{in}$ ratio (well above 1) indicates that soil dissolution potential for that chemical is high, because the output significantly exceeds the input. In Run 1, this rate is highest for Mg^{2+} . It is also high for K^+ , followed by Cl^- , followed by SO_4^{2-} , Na^+ and Ca^{2+} that have similar $\Delta M/M_{in}$ ratios of around 4. A $\Delta M/M_{in}$ ratio of around 1 indicates that M_{out} is significantly low and that the vast majority of input precipitation was retained in the soil. This is the case only for F^- . A $\Delta M/M_{in}$ ratio close to zero means that the mass either retained or released by soil is insignificant compared to the amount input by precipitation. Br^- and NO_3^{2-} have a $\Delta M/M_{in}$ close to zero.

$\Delta M/\Delta t$ is the mass rate of release (if positive) or retention (if negative) of a species in units of $\mu g/min$. Higher positive number indicates faster rate of release and higher negative number indicates faster rate of retention. SO_4^{2-} had the faster rate of release and F^- had the fastest rate of retention.

Run 2 Observations

Largely positive ΔM values were yielded for Mg^{2+} , K^+ , Cl^- , and Ca^{2+} , because of a combination of 2 factors: First, actual 20X concentrated input measured to be lower than intended, making overall M_{in} not significantly large, and secondly, these species were able to dissolve out significantly like they did in Run 1, making a large M_{out} . For Br^- , M_{in} for Run 2 was close to Run 1, because 20X concentration was not successfully achieved. M_{out} for Br^- in Run 2 increased and yielded a positive ΔM , which is higher than the ΔM value from Run 1, which was near zero for Br^- . In Run 2, F^- and NO_3^{2-} , as well as SO_4^{2-} and Na^+ , maintained highly negative ΔM values. This difference from the previous Run was due to highly concentrated 20X input, making M_{in} very high. In Run 1, dissolved soil was the major source of SO_4^{2-} and Na^+ , but in Run 2, soil was not able to reach a level of dissolution to exceed the highly concentrated rainwater input. This indicates that there is an equilibrium value that soil dissolution reaches.

The same species that had highly positive $\Delta M/M_{in}$ ratios for Run 1 were the ones that stayed positive, because these are the species where soil dissolution rates are high, and output mass significantly

exceeds the input. In Run 1, SO_4^{2-} and Na^+ had the lowest positive $\Delta\text{M}/\text{M}_{\text{in}}$ ratios, and in Run 2, they became slightly negative for same above mentioned reasons.

Rates of dissolution (indicated by $\Delta\text{M}/\Delta\text{t}$ in $\mu\text{g}/\text{min}$) for species Cl^- , Mg^{2+} , Ca^{2+} and K^+ have not changed much from R1 to R2. $\Delta\text{M}/\Delta\text{t}$ decreased to slightly negative rate values for SO_4^{2-} and Na^+ , since they have switched from dissolving to retained species in Run 2, whereas it increased to slightly positive value for Br^- since it switched from a retaining to dissolving species. $\Delta\text{M}/\Delta\text{t}$ rate became significantly more negative in Run 2 for NO_3^{2-} , indicating faster rate of retention, whereas it became less negative for F^- , indicating slower rate of retention.

Soil Leaching Batch Experiments

Table 7 summarizes batch experiment results. Rain water yielded a higher load of species than DI water. In general, 18 hour samples and 2 hours samples leached out similar load of each species, except for SO_4^{2-} , which dissolved significantly more in 18 hour samples.

Table 7: Batch Experiment Results

	F^-	Br^-	Cl^-	NO_3^{2-}	SO_4^{2-}	Mg^{2+}	Na^+	Ca^{2+}	K^+
DI_2hour	0.07	0.06	0.91	0.81	3.44	0.28	0.72	0.37	1.69
DI_18hour	0.04	0.05	1.03	0.74	4.88	0.29	0.75	0.84	1.75
RW_2hour	n/a	0.11	1.15	1.50	4.33	0.35	0.86	0.41	2.09
RW_18hour	n/a	0.08	0.97	1.20	4.75	0.37	1.03	0.43	1.90
(RW18hr) - Cp	n/a	0.04	0.59	0.27	3.82	0.33	0.83	0.31	1.85
Dissolved/ MassSoil*	-8.3E- 07	4.4E- 07	5.9E- 06	2.7E- 06	3.8E- 05	3.3E- 06	8.3E- 06	3.1E- 06	1.9E- 05

$$*\frac{\text{Dissolved}}{\text{MassSoil}} = \frac{\text{g leached}}{\text{g soil}} = \frac{(\text{RW18hr}^{**} - \text{Cp}) \frac{\text{mg}}{\text{L}} \times 10 \text{ ml} \times \frac{1}{10^6}}{1 \text{ g soil}}$$

**Output concentration of 18 hour RW batch results were used (in 5th row of Table 7) as they seemed most appropriate to the experiment that lasted for days, where the soil was able to interact with soil for that long.

M_{soil} : M_{water} Ratio

Batch Experiment- 1:10

Model Experiment- 40:10

$$\frac{7584 \text{ g}}{1908 \text{ mL pore}} \times \frac{1 \text{ mL pore}}{1 \text{ mL water}} \times \frac{1 \text{ mL water}}{1 \text{ g water}} = 4:1 \text{ ratio} = 40:10 \text{ ratio}$$

These values from are from Table 2, and making the assumption that 1 mL pore volume interacts with 1 mL water, or assuming full saturation (for rough estimate only).

From this calculation, it is assumed that model experiment load is expected to be 40 times concentrated than batch load. From Table 7, it can be seen that dissolved load per mass unit of soil is highest for SO_4^{2-} , followed by K^- . The species Cl^- , Mg^+ , Ca^{2+} , Na^+ as well as NO_3^{2-} all have one order of magnitude smaller dissolved/soil ratio. Br^- has one more order of magnitude smaller dissolved/soil ratio, and F^- has a negative ratio. For species SO_4^{2-} , K^- , Cl^- , Mg^+ , Ca^{2+} and Na^+ , these values make sense because positive values indicate that soil dissolves these chemicals. For NO_3^{2-} and Br^- , these values were expected to be negative or low, because soil in the experiment typically retained these species. Retention of these species did not occur in the batch experiments, probably because the soil mass concentration is approximated to be 40 times higher in the experiment than in the batch experiments. If batch experiment were done with an appropriate and higher $\text{M}_{\text{soil}}:\text{M}_{\text{water}}$ ratio, soil would have better and more opportunities to retain NO_3^{2-} and Br^- . Dissolved per mass soil ratio was negative for F^- as expected. Due to the soil's high retention capacity for F^- , retention was able to take place regardless of lower $\text{M}_{\text{soil}}:\text{M}_{\text{water}}$ ratio in the batch experiments.

Discharge Data

Figure 17 and Figure 20 are the graphs of actual flow rate and concentration of each species in both precipitation and in output, all against time. In Figure 20, note that for both Runs, there was no DOC present in input rainwater, and pH was around 5. Figure 18 gives all the graphs of aforementioned ratios V_d/V_p (Ratio_V), Ratio_{TV} and Ratio_C , for each species over time.

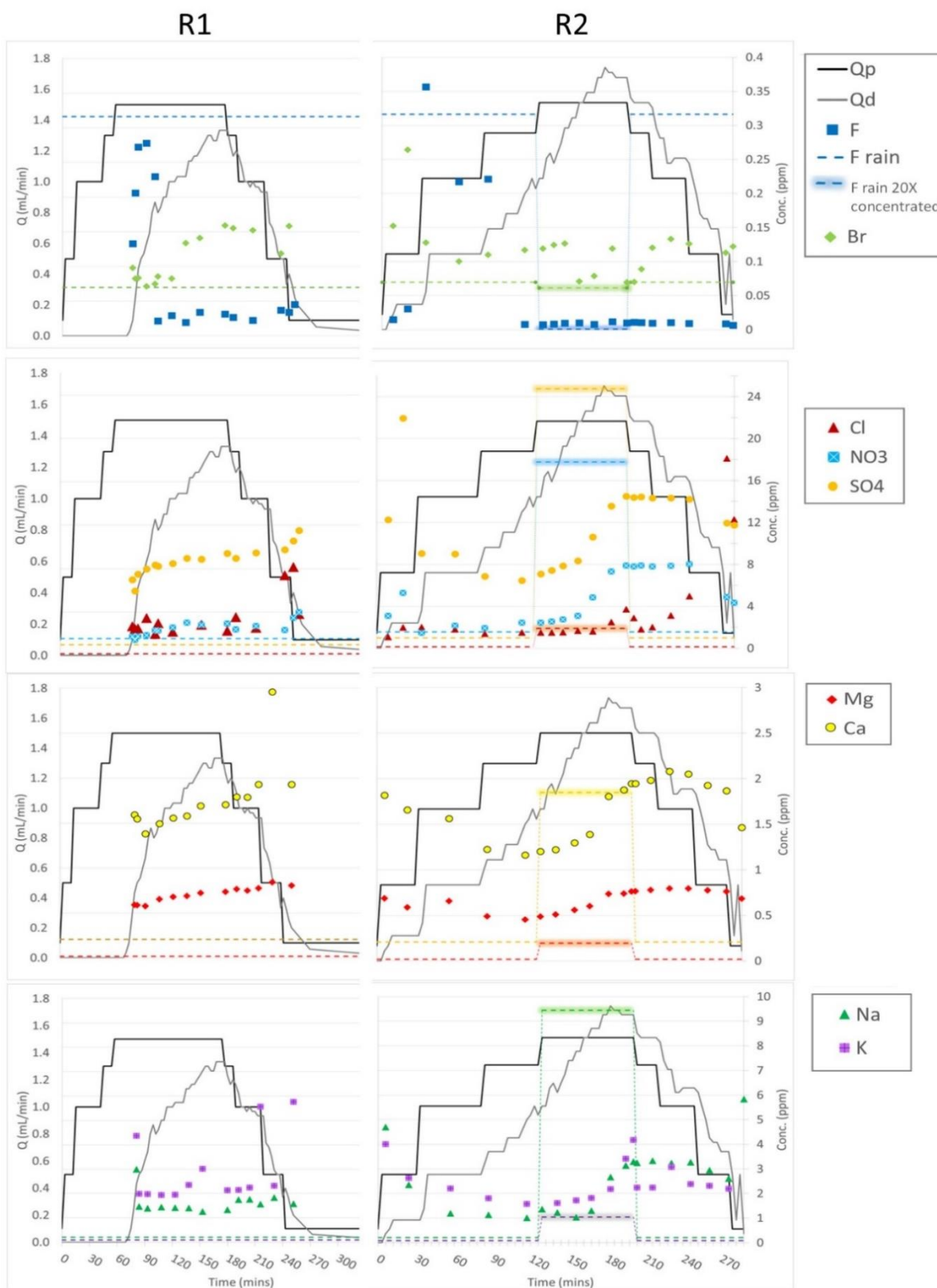


Figure 17: C and Q (horizontal gridlines are for Conc. right axis)

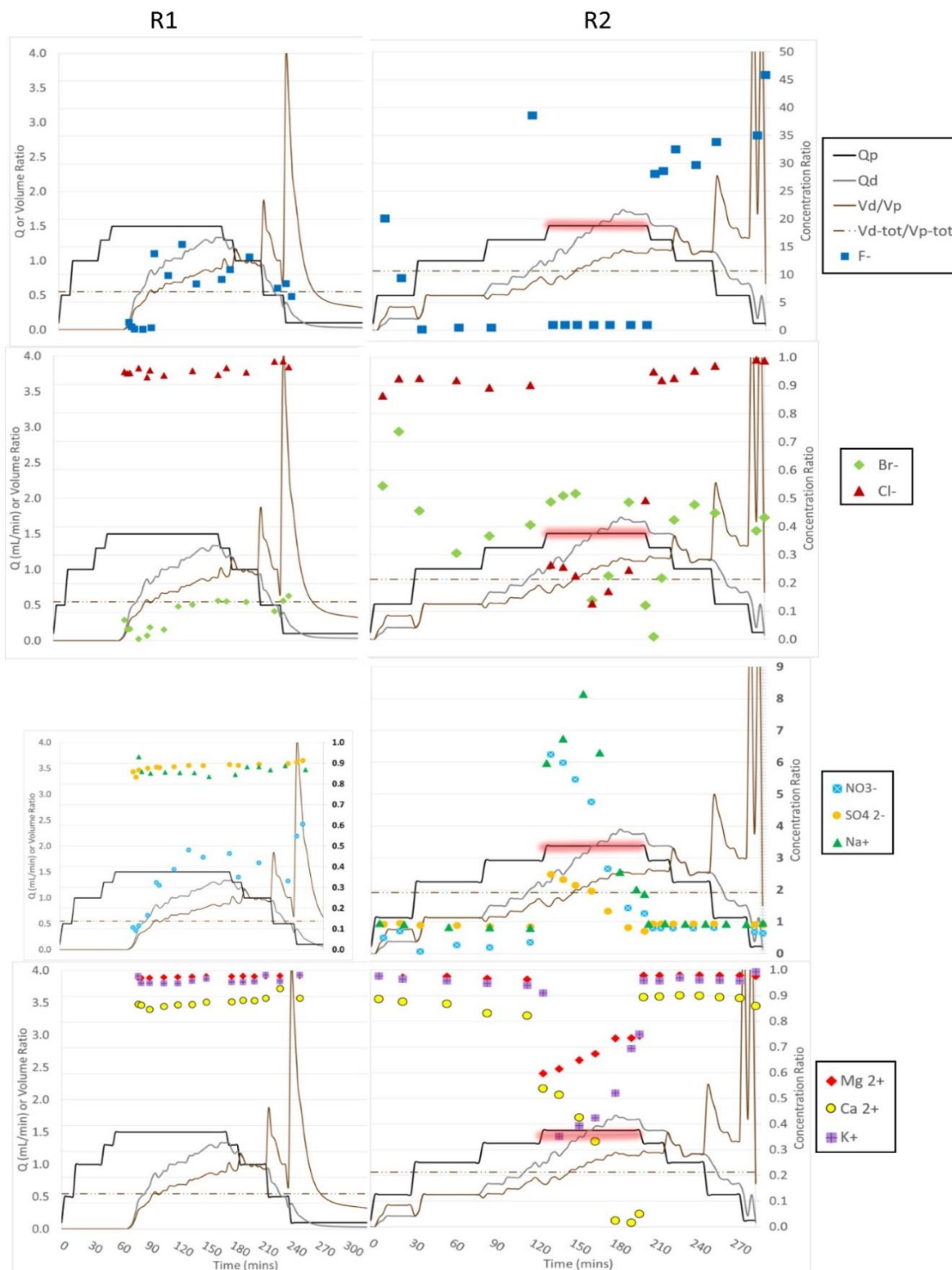


Figure 18: Ratios and Q (horizontal gridlines are for Conc. right axis)

Ratio_v (Volume Ratio) increases slightly over time for both runs partly because at the initial stage, pores in the catchment are still being filled and discharge is still starting to form. With time, more of the input becomes output. On the other hand, Ratio_C (Concentration Ratio) characterizes the old water contribution to discharge load. In these graphs, the response of Q_d curve to Q_p can be contrasted from Run 1 to Run 2. For R1, there was a larger time lag between the appearances of Q_d after Q_p starts, as pores were less saturated and incoming water infiltrated to fill pore space before forming saturated lateral flow. For R2, there was a shorter time lag because saturation increased, and discharge became easier to form. For R2, Q_d more easily and more prominently exceeded Q_p during the falling limb, because of loss of infiltration due to oversaturation.

Run 1 Observations

Fluoride

As seen in Figure 17, C_d of F^- decreased with time. C_d of F^- started slightly lower than C_p in the beginning, and decreased more significantly along the rising limb of Q_d , discharge. In Figure 18, Ratio_C is below 1 at first, then jumps toward high value of 15, which is where C_d also decreases suddenly. In the beginning when Ratio_C is slightly higher than 1, C_p contributes largely to C_d . The sudden decrease in C_d when Ratio_C increases to well above 1 maybe because, as Run 1 continues, old water contribution increases as pore spaces get connected and increase the overall buffering capacity of old water, which ultimately lowers $[F^-]$ in the discharge. The buffering capacity may be due to sorption of F^- onto the soil matrix.

Bromide and Nitrate

In Run 1, Both Ratio_C and C_d of Br⁻ and NO₃²⁻ slightly follow the V_d/V_p curve. C_d starts off closer to C_p at the rising limb, which explains Ratio_C close to 0. Over time, Ratio_C increases but stays well below 1, meaning soil leachate containing Br and NO₃ are contributing to the discharge along with the input rain, and that mixing is involved. Gradual increase in Ratio_C means that, with time, overland flow contribution becomes less significant as old-water and soil-interface contribution becomes more important. This verifies the claim made above in the Fluoride discussion that old water channels form with time as more and more pore spaces get connected. One difference is that C_d of Br⁻ increases and diverts from C_p more than NO₃²⁻ does.

Again with 20X rain water in Run 2, there was no [Br⁻] in the recipe, and the 20X measured concentration turned out to be very close to the 1X concentration, rendering the 20X observations not very useful. Again in Run 2, more chaotic behavior is seen, perhaps due to excess saturation of pores compared to Run 1.

Chloride, Sulfate, Magnesium, Calcium, Sodium and Potassium

For all of these species in Run 1, Ratio_C is consistently close to 1, and C_d is well above C_p, meaning soil is the main source of the chemical load. All these species (except Na⁺ and Mg²⁺ only slightly), C_d increases along both the rising and falling limbs, without change in Ratio_C. C_d of SO₄²⁻, Mg⁺, Ca²⁺ started higher than C_p, and increased with time. C_d of Na⁺ and K⁺ also started higher than C_p, but only increased slightly over time. For Cl⁻, C_d close to C_p and increased only slightly over time.

Sulfate C_d has a prominent shape resembling $y=x^3$ function along Q_d. This could again indicate that over the course of Run 1, channels for old water to potentially travel through became more connected and ready to release higher load of these chemicals overall. This trend and the fact that sulfate maintained

highly negative ΔM values also indicate that the watershed may be maximizing its dissolution load by releasing the stored mass first, and then taking in more sulfate later.

Run 2 Observations

In R2, C_d of each species' during 1X concentrated C_p parts, were similar to C_d values of R1. Actual 20X rain water turned out to not have 20 times 1X concentration rain water as intended. For the species NO_3^{2-} , SO_4^{2-} , Na^+ , Mg^+ , Ca^{2+} and K^+ for which higher C_p was achieved, C_d increased in response to 20X C_p . For species that 20X C_p value did not actually change much from 1X C_p (F^- and Br^-), C_d did not increase in response to 20X C_p as expected.

For the 20X injection, there was no $[\text{F}^-]$ in the rain water. C_d along the rising limb of Run 2 is slightly chaotic. Before 20X RW is injected, C_d is low around 0, then hovers around C_p , and comes back down to near 0. Old water contributes when C_d is low, but when Ratio C is close to 0, overland flow dominates for some time, but is transient in this case. When the 20X C_p is reduced to near 0, C_d is consistently near 0. Because Ratio_C is also near 0, it is safe to say that overland flow, not old-water, has a large contribution in this stage. However, when R_c increases again after the injection is switched to 1X C_p , it means that old water should be having a large contribution again. However, in Figure 17, it is observed that C_d still stays consistently near 0 till the end of Run 2. This means that there is a high mixing and buffering capacity in the old water which retains a low $[\text{F}^-]$ despite C_p being as high as 0.3 ppm when the injection is switched back to 1X concentration. It also implies that old water channels take time to form to create pathways that start from rainfall going into the discharge stream.

For Run 1 in Figure 18, most species had Ratio_C of around 1 except, F^- whose Ratio_C is higher than 1, and Bromide and Nitrate, whose Ratio_C is lower than 1. In Run 2, the Ratio_C levels stay at the same levels. However, when 20X rainwater is injected, Ratio_C spikes up and down before it stabilizes again at a certain level after input is switched back to 1X. The different responses to 20X C_p seem to fit

into three patterns with RatioC vs time. During the 20X injection, Rc behaved in one of three ways, as indicated in Figure 19:

Pattern A (green): spiked up to >1 and gradually decreased back to 1

Pattern B (red): gradually decreased to zero before spiking up

Pattern C (blue): spiked to <1 level before gradually decreasing

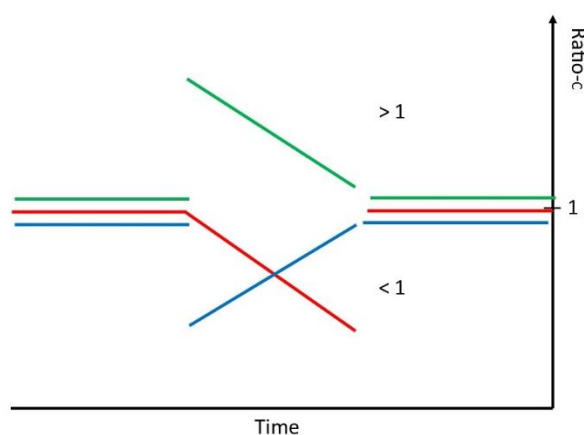


Figure 19: 20X Ratio-C Patterns

Pattern A: Sulfate, Sodium (and Nitrate)

20X concentration was significantly higher than C_d at 1X injection. Therefore, C_p started gaining more influence and spiked Rc. But even as 20X injection continued steadily, Rc started to approach 1 while C_d approached a higher level. This means soil water composition quickly synchronized itself to 20X input, and was able to release higher C_d . When the input was changed to 1X, $R_c = 1$ and C_p had little influence. However, C_d managed to stay at the previous high levels for 50 minutes after this switch, before decreasing to its normal levels. This indicates that although C_p influence stopped when 20X input was stopped, there was significant amounts of 20X RW stored as old water and slowly released through connected subsurface pathways.

Pattern B: Calcium

Calcium 20X concentration resembled C_d at 1X input, and therefore Rc approaches to 0, before spiking back to soil influence only after 1X injection is used.

Pattern C: Magnesium, Potassium

20X concentration was only increased slightly, and therefore C_d only increased slightly. C_p gained more influence because it was close to C_d in this case. As 20X influence continued, R_c approached 1 before stabilizing at 1 immediately after switching to 1X input. This again means that soil water gained the composition of 20X C_p and started influencing C_d more and more.

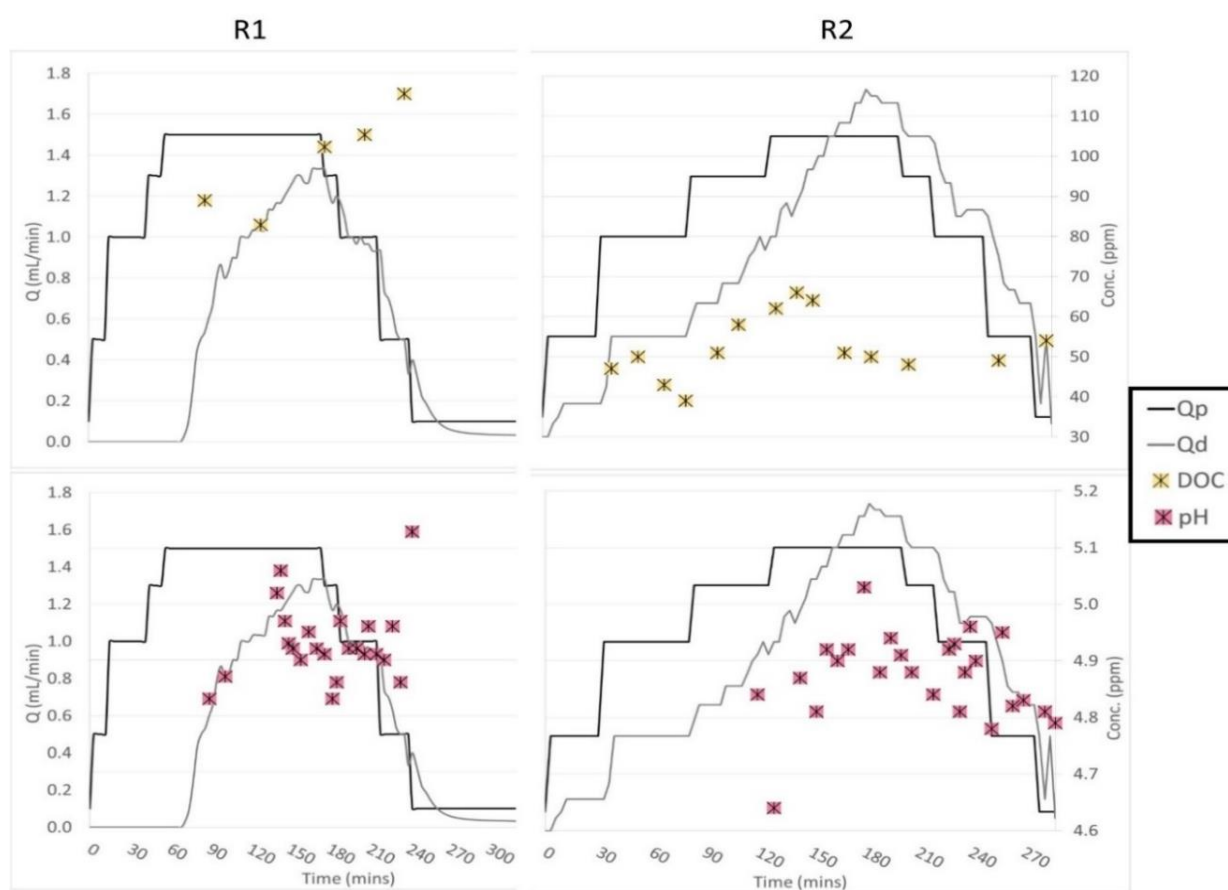


Figure 20: C and Q –part 2 (horizontal gridlines are for Conc. right axis).

DOC and pH

These species are analyzed separately from the rest of the species because of the differing amounts of samples and range of values. DOC somewhat followed discharge curve –increased on rising and decreased on falling limb. pH also slightly increased on rising and decreased on falling limb. pH of

rainfall is ~5, so therefore soil leached out some acidic load. DOC was significantly lower in Run 2 than in Run 1, meaning it washed out over time. pH was also slightly lower overall in Run 2 than in Run 1 without the rainfall pH changing. Lower pH indicates higher dissolution of H⁺ ions. This could have happened as 20X C_p in R2 released many species that attached to soil colloids, pushing more H⁺ into solution.

End Member Mixing Analysis

Table 8: Calculations/Values for Mixing Diagram

Graph in Figure 21	[ppm]	x	y
I)		SO ₄ ²⁻	F ⁻
	C _p	0.93	0.32
	SoilW	152.90	0.00
II)		Ca ²⁺	NO ₃ ²⁻
	C _p	0.20	0.93
	SoilW	33.00	10.80
III)		Na ⁺	Br ⁻
	C _p	0.12	0.03
	SoilW	12.40	1.70

Table 8 gives the x and y coordinate values used to plot the straight lines in Figure 21. C_p is the concentration in one end-member, rainwater, and SoilW is the predicted load of the species coming from soil leachate. SoilW were calculated from 18 hour RW batch experiment, by taking the batch experiment results and subtracting rainwater concentration from it. A line from end member 1 (C_p) to end member 2 (soil water) indicates that the overall load shifts from one to the other over time. The plotted dots (C_d) agree with the direction of the line. As Run 1 continues, outlet concentration of each chemical yields to the soil water, or old water composition. This indicates that old water contribution to discharge increases over time.

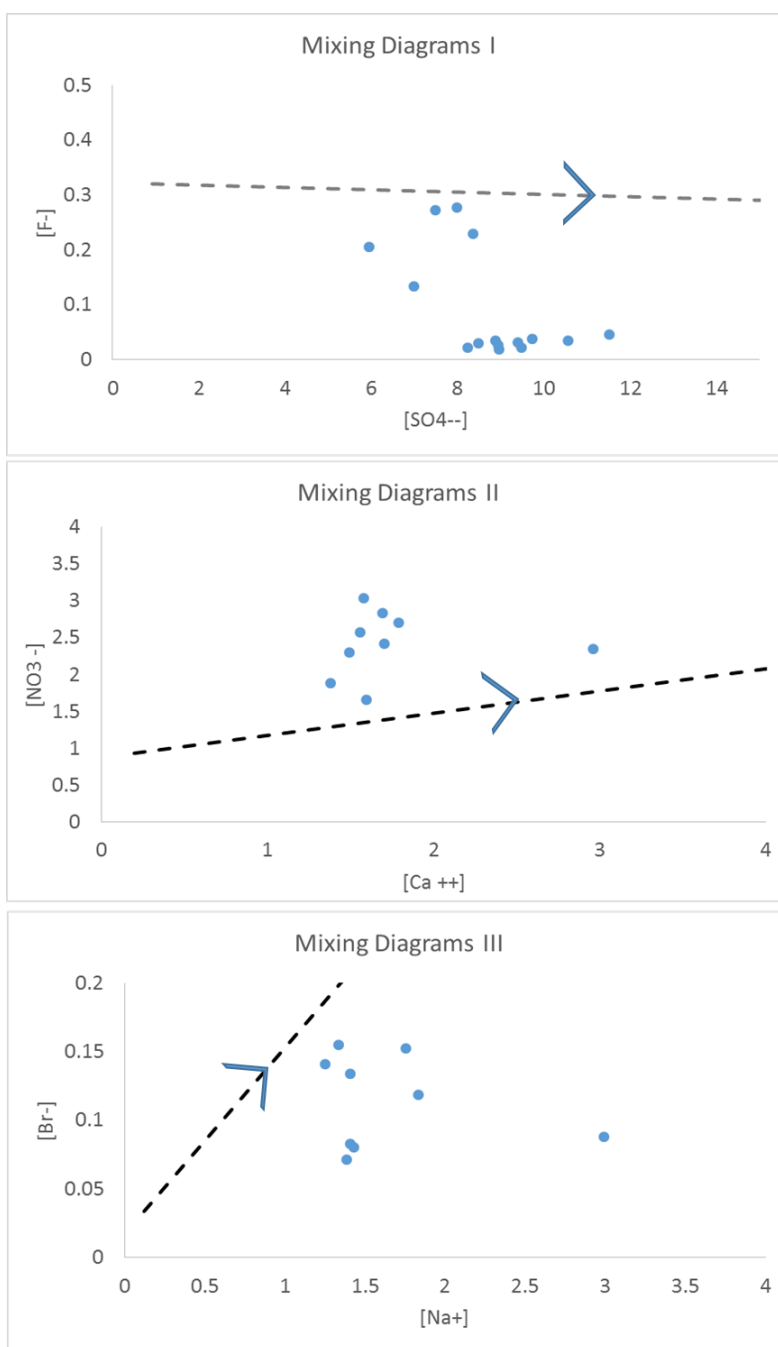


Figure 21: 1-dimensional EMMA for Run 1

Hysteresis Patterns

Figure 22 gives the graphs of C_d against Q_d for Run 1 only. These hysteresis loops can roughly reveal properties of how chemical load responds in a stream, also summarized in Table 9.

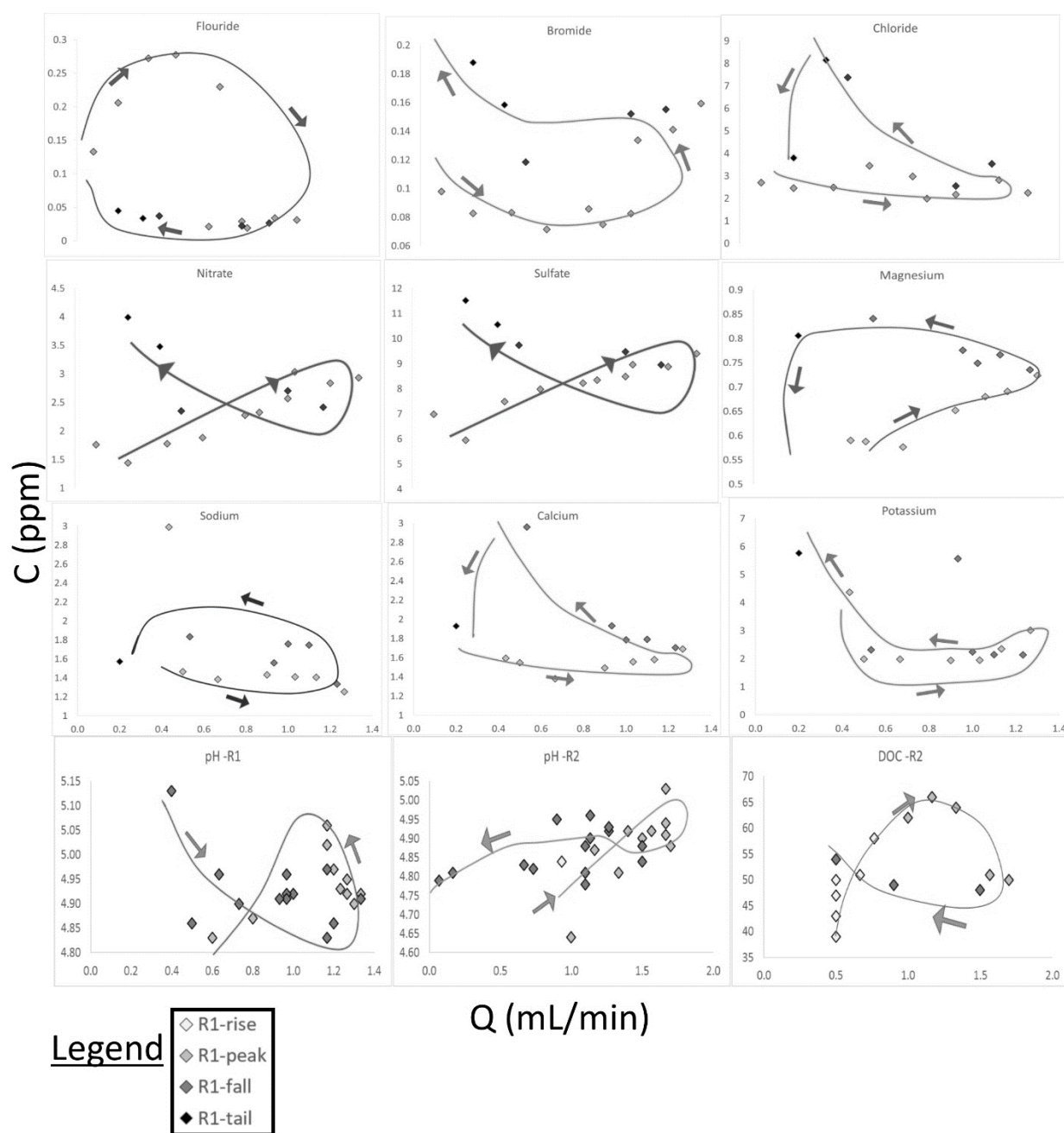


Figure 22: C-Q Graphs -Hysteresis Loops

Table 9: Hysteresis Summary

	F ⁻	Br ⁻	Cl ⁻	NO ₃ ²⁻	SO ₄ ²⁻	Mg ²⁺
Pattern	2 or 1	4		1, 2 Crisscross		3 or 4
Meaning	C _d ↓ t Chemodynamic	C _d ↑ t C _p < C _{old} Dilution		C _d ↓ ↑ t Both dilution and chemodynamic behavior		C _d ↑ t Chemostatic
	Na ⁺	Ca ²⁺	K ⁺	pH-R1	pH-R2	DOC
Pattern	4 or 3	4		Inconclusive		1, 2
Meaning	C _d ↑ t Chemostatic	C _d ↑ t C _p < C _{old} Dilution				C _d ↓ t Both dilution and chemodynamic

Br⁻, Cl⁻, Ca²⁺ and K⁺ exhibit counter-clockwise pattern 4, meaning their C_d increase with time, and C_{old} is more significant than C_p. This is proven to be true from Figure 17 and above discussions concluding that these species get dissolved into solution when contacted with rain water. Although, the dissolution of Br⁻ was not significant in magnitude. Br⁻, Cl⁻, Ca²⁺ and K⁺ in general decrease with increased discharge and exhibit rough dilution behavior. NO₃²⁻ and SO₄²⁻ exhibit a crisscross CQ pattern resembling both Patterns 1 and 2. However, in Figure 17 it can be observed that these species increase slightly with time. Nevertheless, the crisscross pattern indicates that these is both chemodynamic and dilution behavior present, which is typically the case with species related to organic matter. DOC and F⁻ exhibit clockwise patterns indicating that Cd decreased over time, which can be seen clearly in Figure 17 and Figure 20. F⁻ falls into the chemodynamic category while DOC is variant. Mg²⁺ and Na⁺ on the other hand, are roughly the shape of Pattern 3 or 4, but it is uncertain. Clearly, there are significant amounts of these species leaching out from the soil, and soil water was analyzed to be the major end-member before for this species, leading to the conclusion that C_p < C_{old}. Mg²⁺ and Na⁺ can be categorized as chemostatic species, possibly because of high intrinsic weathering rates that are not affected by discharge rate. For the

most part, $C_p < C_{old}$ which verifies our previous claims that old water contribution in the experiment was significant, especially as time went on.

Classification

Characteristics discussed above allow the species to be categorized. Type A is species where discharge load is smaller than the input rainfall load. This means that rain water has significant influence on discharge load but soil does not significantly leach out this chemical, and therefore buffers (lowers) the dissolved discharge load. Type B is species where discharge load is similar to input load, therefore soil is not leaching out much of this. Type C is species that derives mainly from soil because rain water composition is not significant. In Table 5, $\Delta M/Min$ ratio is close to 1 for Type A, close to 0 for Type B, and negative for Type C.

Table 10: Experiment Observations Summary

	F ⁻	Br ⁻	Cl ⁻	NO ₃ ²⁻	SO ₄ ²⁻	Mg ²⁺	Na ⁺	Ca ²⁺	K ⁺	DOC	pH
Retention(R)/ Dissolution(D) / Neutral(N)	R	N	D	R	D	D	D	D	D	D	N
R/D capacity*	high	none	high	low	low	high	low	high	high	high	
R/D rate*	high	none	medium	high	high	low	low	low	medium	high**	
Q _p effect	chemodynamic	dilution		crisscross		chemostatic		dilution		crisscross	chemostatic
Rc	>>1	< 1	~1	< 1	~1						<=1
Type	A	B	C	B	C						

*observations from Tables 5 and 6

**DOC decreased significantly over time

As seen in Table 10, there are a multitude of varying behaviors for each chemical species, in terms of method of travel from precipitation to discharge from stream mouth, how soil retains or dissolves this species, and in terms of how end members interact to influence its CQ relations, if they do. Species

with high rates of either retention or dissolution (such as NO_3^{2-} , SO_4^{2-} and DOC) showed crisscross CQ patterns. It was noted in the introduction section that species derived primarily from fast weathering, are affected less by discharge changes [Ameli, 2017], and therefore, it makes sense that there is no distinctive CQ relationship. However, Mg^{2+} and Na^+ had lower rates of dissolution, comparatively, and also showed little correlation with discharge.

Species with high R/D potential but low to medium R/D rates (Cl^- , Ca^{2+} , K^+) showed dilution behavior, which may be because although high flow rate would potentially drive excessive dissolved load from soil to stream, the chemical rate of species release is not able to keep up with the physical push by increased discharge. Br^- shows interesting behaviors, as it typically did not release or retain a large load into the discharge stream and rain water passed through. Typically, conservative tracers tends to be a chemical such as Cl^- instead, which was not the case here.

Chapter 4 : CONCLUSION

Nine major species measured here are characterized into one of three categories in terms of how the species is transported into the stream. Fluoride belongs to Type A where rain water is the major source and soil acts to retain it from entering the stream discharge. Bromide and nitrate exhibit Type B behavior where both end members of soil and rain contribute to the stream water and the magnitude of the contribution is compatible. All other species (Chloride, Sulfate, Magnesium, Calcium, Sodium and Potassium) are Type C where soil water is so dominant that it is the significant end member. Most of these species exhibit Type C behavior, which leads to further analysis. In this experiment, the rain simulations replicated heavy intensity and large-volume rain fall events of real life, and could lead to future research on whether such events lead to predominantly type C behavior in chemical load. It was also found that species that have a high dissolution rate do not fit into a CQ relation pattern, but those of the Type C species that have slower dissolution rates tend to exhibit rough CQ patterns (dilution or chemodynamic).

Due to constraints on time and scope of the undergrad research thesis, there are several missing pieces that further characterize end members and nutrient transport. Certain values such as saturation, water content in the soil and measurement of soil water composition would have made this analysis both more accurate and broader. One question is whether the Type 1 species, such as fluoride that are lower in concentration in the output than the input, are behaving so due to soil-interfacial phenomenon such as adsorption? How does CEC (cation exchange capacity) help explain the large amount of cation dissolution observed in the experiment?

BIBLIOGRAPHY

- Allan, J.D. 1995. *Stream Ecology: Structure and Function of Running Waters*. Chapman & Hall, London, 388 p.
- Ameli, A. A., Beven, K., Erlandsson, M., Creed, I. F., McDonnell, J. J., & Bishop, K. (2017). Primary weathering rates, water transit times, and concentration-discharge relations: A theoretical analysis for the critical zone. *Water Resources Research*, 53(1), 942-960. doi:10.1002/2016WR019448
- Anderson, S. P. D., William E.; Torres, R. (1997). Concentration-discharge relationships in runoff from a steep, unchanneled catchment. *Water Resources Research* 33(1): 211-225.
- “Annual Findings.” CZO -Critical Zone Observatory: Studying the zone where rock meets life. *NSF - National Science Foundation*. <http://criticalzone.org/shale-hills/research/annual-findings-shale-hills/>
- Bao, C.; Yuning S.; Li L.; Duffy C. (2016). Understanding Hydrogeochemical Processes at the Watershed Scale: 1. Development of RT-Flux-PIHM.; Manuscript In: John and Willie Leone Department of Energy and Mineral Engineering, The Pennsylvania State University, University Park, PA 16802
- Basu, N., Destouni, G., Jawitz, J., Thompson, S., Loukinova, N., Darracq, A., Rao, P. (2010). Nutrient loads exported from managed catchments reveal emergent biogeochemical stationarity. *Geophysical Research Letters*, 37(23), n/a. doi:10.1029/2010GL045168
- Berner, E.K., R.A. Berner. 1987. *The Global Water Cycle: Geochemistry and Environment*. Prentice Hall, Engle-wood Cliffs, NJ, 397 p.
- Bracken, L. J. and J. Croke (2007). The concept of hydrological connectivity and its contribution to understanding runoff-dominated geomorphic systems. *Hydrological Processes* 21(13): 1749-1763.
- Clow, D. W. and M. A. Mast (2010). Mechanisms for chemostatic behavior in catchments: Implications for CO₂ consumption by mineral weathering. *Chemical Geology* 269(1-2): 40-51.

- Evans, C. and T. D. Davies (1998). Causes of concentration/discharge hysteresis and its potential as a tool for analysis of episode hydrochemistry. *Water Resources Research* 34(1): 129-137.
- “Floods and droughts” Fourth Assessment Report: Climate Change 2007; Intergovernmental Panel on Climate Change. https://www.ipcc.ch/publications_and_data/ar4/wg2/en/ch3s3-4-3.html
- Grimm, N. B., Gergel, S. E., McDowell, W. H., Boyer, E. W., Dent, C. L., Groffman, P., Pinay, G. (2003). Merging aquatic and terrestrial perspectives of nutrient biogeochemistry. *Oecologia*, 137(4), 485-501. doi:10.1007/s00442-003-1382-5
- Herndon, E. M., Dere, A. L., Sullivan, P. L., Norris, D., Reynolds, B., & Brantley, S. L. (2015). Biotic controls on solute distribution and transport in headwater catchments. *Hydrology and Earth System Sciences Discussions* 12(1): 213-243.
- Hooper, R. C.; Peters, N. (1990). Modeling streamwater chemistry as a mixture of soilwater endmembers -An application to the Panola Mountain Catchment, Georgia, USA. *Journal of Hydrology* 116: 321-343.
- Hornberger, G. M. 2014. *Elements of physical hydrology*. 2nd ed. Baltimore, Md: Johns Hopkins University Press.
- Jencso, K. G., McGlynn, B. L., Gooseff, M. N., Wondzell, S. M., Bencala, K. E., & Marshall, L. A. (2009). Hydrologic connectivity between landscapes and streams: Transferring reach- and plot-scale understanding to the catchment scale. *Water Resources Research*, 45(4), W04428. doi:10.1029/2008WR007225
- Johnson, N. B., F. H.; Fisher, D.W.; Pierce, R. S. (1969). A Working Model the Variation in Stream Water Chemistry at the Hubbard Brook Experimental Forest, New Hampshire. *Water Resources Research* 5(6).
- Kirchner, J. F., Xiahong; Neal, C. (2001). Catchment-scale advection and dispersion as a mechanism for fractal scaling in stream tracer concentration. *Journal of Hydrology* 254: 82-101.

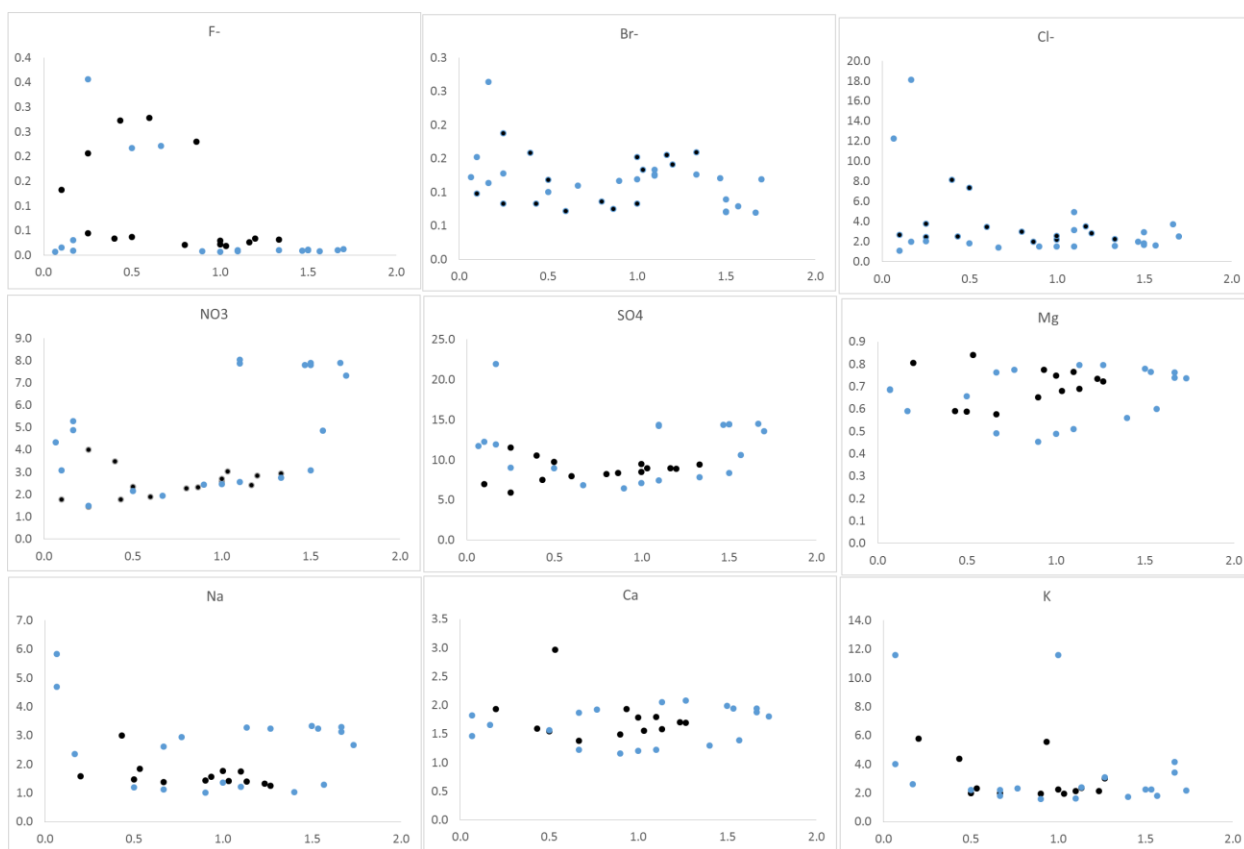
- McDiffett, W. F. B., Andrew W.; Dominick, T. F.; Kenneth D. (1989). Nutrient concentration-stream discharge relationships during storm events in a first-order stream. *Hydrobiologia* 179: 97-102.
- McGuire, K. J., McDonnell, J. J., Weiler, M., Kendall, C., McGlynn, B. L., Welker, J. M., & Seibert, J. (2005). The role of topography on catchment-scale water residence time. *Water Resources Research* 41(5): doi:10.1029/2004WR003657
- Sebestyen, S. D., E. W. Boyer, J. B. Shanley, C. Kendall, D. H. Doctor, G. R. Aiken, and N. Ohte (2008), Sources, transformations, and hydrological processes that control stream nitrate and dissolved organic matter concentrations during snowmelt in an upland forest, *Water Resources Research*, 44(12).
- Stallard, R. F. M., Sheila F. (2014). A Unified Assessment of Hydrologic and Biogeochemical Responses in Research Watersheds in Eastern Puerto Rico Using Runoff–Concentration Relations. *Aquat Geochem* 20: 115-139.
- Swiss Standard SN 670 010b, Characteristic Coefficients of soils, Association of Swiss Road and Traffic Engineers
- Sverdrup, H.; Warfvinge P. (1993), Calculating field weathering rates using a mechanistic geochemical model PROFILE, *Appl. Geochem.*, 8(3), 273–283.
- Thurman, E.M. 1985. *Organic Geochemistry of Natural Waters*. Martinus Nijhoff/Dr W Junk, Dordrecht, The Netherlands, 497 p.
- Walling, D.E., B.W. Webb. 1986. Solutes in river systems. In: S.T. Trudgill, ed., *Solute Processes*. John Wiley & Sons, Chichester, pp. 251-327
- Williams, G. P. (1989). Sediment concentration versus water discharge during single hydrologic events in rivers. *Journal of Hydrology* 111: 89-106.
- Wohl, Ellen 2014. *Rivers in the landscape: Science and management*. 1st ed. Hoboken, NJ;Chichester, West Sussex;: John Wiley & Sons Inc.

APPENDIX

Below is the C vs Q plots for Run 1 and 2 for each chemical. Since Run 2 had 20X concentrated input for only the middle part of the Run, it was anticipated to yield higher C levels at higher Q levels, skewing only the right part of each graph. This seems to be true for the species where 20X C_p was actually significantly higher than 1X. It was concluded that the partial skew of the graph would limit the understanding on CQ hysteresis, and therefore was not used in the experimental analysis.

● R1

● R2



ACADEMIC VITA

Sruthi Kakuturu
sruthikakuturu94@gmail.com

Education

Major: Bachelor of Science, Environmental Systems Engineering

Honors: Environmental Systems Engineering

Thesis Title: Concentration-Discharge Relations In Connection With End-Members and Flow Paths, In a Model Catchment

Thesis Supervisor: Li Li

Work Experience

Date: January –December 2016

Title: Research Assistant

Description: Collected and test samples. Gathered and analyzed results.

Institution: Pennsylvania State University, State College

Supervisor's Name: Li Li

Awards: Deans List (every semester)

President's Academic Excellence Award (high school)

Presentations: "*Effect of Speedwell Forge Dam Reconstruction on Water Quality*", presented at Geological Society of America Conference

Community Service Involvement: Ronald McDonald House volunteer

AID (Association for India's Development) –volunteer and member

Leadership: Stall Manager for *Taste of India 2017* event by AID

Editor of *Sankalp*, annual magazine of AID

Student Senator: Penn State Harrisburg Student Government Association (SGA)

Language Proficiency: English, Telugu, Hindi and Spanish